MATCHING THE OPTIMAL DENOISER IN POINT CLOUD DIFFUSION WITH (IMPROVED) ROTATIONAL ALIGNMENT

Anonymous authors

Paper under double-blind review

ABSTRACT

Diffusion models are a popular class of generative models trained to reverse a noising process starting from a target data distribution. Training a diffusion model consists of learning how to denoise noisy samples at different noise levels. When training diffusion models for point clouds such as molecules and proteins, there is often no canonical orientation that can be assigned. To capture this symmetry, the true data samples are often augmented by transforming them with random rotations sampled uniformly over SO(3). Then, the denoised predictions are often rotationally aligned via the Kabsch-Umeyama algorithm to the ground truth samples before computing the loss. However, the effect of this alignment step has not been well studied. Here, we show that the optimal denoiser can be expressed in terms of a matrix Fisher distribution over SO(3). Alignment corresponds to sampling the mode of this distribution, and turns out to be the zeroth order approximation for small noise levels, explaining its effectiveness. We build on this perspective to derive better approximators to the optimal denoiser in the limit of small noise. Our experiments highlight that alignment is often a 'good enough' approximation for the noise levels that matter most for training diffusion models.

1 Introduction

Diffusion-based generative models have emerged as a powerful class of generative models for complex distributions in high-dimensional spaces, such as natural images and videos.

Diffusion models operate on the principle of reversing a noising process by learning how to denoise. Let p_x be our data distribution defined over \mathbb{R}^d . Let $p_y(\cdot;\sigma)$ be the distribution of $y=x+\sigma\eta$ where $x\sim p_x,\eta\sim\mathcal{N}(0,\mathbb{I}_d)$. y represents a noisy sample at a particular noise level σ . When the noise level is zero, we have that $p_y(\cdot;\sigma=0)=p_x$, as expected. On the other end, as $\sigma\to\infty$, the data distribution p_x is effectively wiped out by the noise and $p_y(\cdot;\sigma)\to\mathcal{N}(0,\sigma^2\mathbb{I}_d)$. As explained by Karras et al. (2022), the idea of diffusion models is to randomly sample an initial noisy sample $y_M\sim\mathcal{N}(0,\sigma_M^2\mathbb{I}_d)$, where σ_M is some large enough noise level, and sequentially denoise it into samples y_i with noise levels $\sigma_M>\sigma_{M-1}>\dots>\sigma_0=0$ so that at each noise level $y_i\sim p(y;\sigma_i)$. Assuming the denoising process has no error, the endpoint y_0 of this process will be distributed according to p_x .

Many schemes (Song et al., 2022; Yang et al., 2024; Karras et al., 2022) have been built for sampling diffusion models; the details of which are not relevant here. The essential component across these is that one trains a denoiser model D that minimizes the denoising loss $l_{\rm denoise}$ across noisy samples at a range of noise levels:

$$\min_{D} l_{\text{denoise}}(D) = \min_{D} \mathbb{E}_{x \sim p_x} \mathbb{E}_{\eta \sim p_\eta} \mathbb{E}_{\sigma \sim p_\sigma} [\|D(x + \sigma \eta; \sigma) - x\|^2]$$
 (1)

Once learned, the denoiser model D is then used to iteratively sample the next y_i from y_{i+1} using a numerical integration scheme, such as the DDIM update rule (Song et al., 2022) (for example):

$$y_i = y_{i+1} + \left(1 - \frac{\sigma_i}{\sigma_{i+1}}\right) \left(D(y_{i+1}, \sigma_{i+1}) - y_{i+1}\right)$$
 (2)

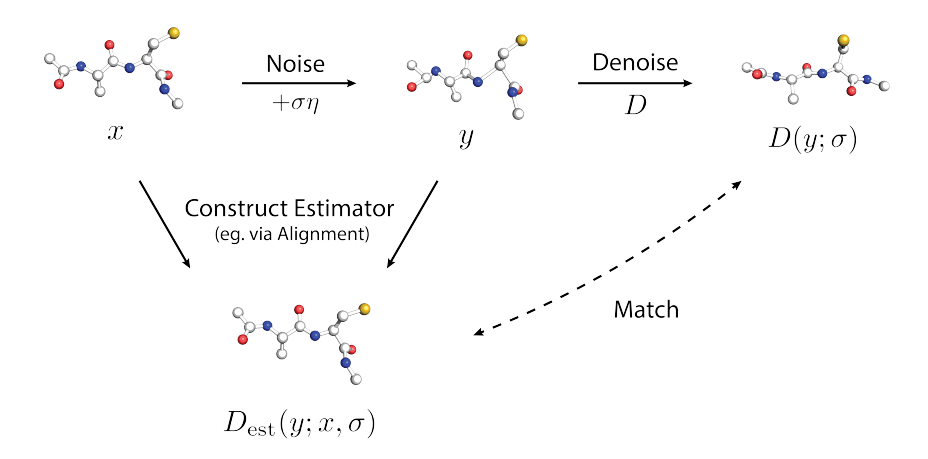


Figure 1: Overview of the training process of a denoising diffusion model, represented by D. A sample point cloud x is first noised to give y. D denoises y to give a new point cloud $D(y;\sigma)$, which gets matched to an estimator $D_{\text{est}}(y;x,\sigma)$ of the optimal denoiser D^* . The usual estimator is $D_{\text{est}}(y;x,\sigma)=x$. Here, we show that rotational alignment gives rise to better estimators of D^* .

We are particularly interested in the setting where the data samples naturally live in three-dimensional space, such as molecular conformations, protein structures and point clouds. Often in these settings, there is no canonical 3D orientation that can be assigned to the data samples. Thus, we would like to sample all orientations of the data samples with equal probability. Formally, this means that our 'true' data distribution is $\operatorname{Aug}[p_x]$, where each sample $x \sim p_x$ has been augmented with uniformly sampled rotations $\mathbf{R} \in SO(3)$.

There are two main approaches to obtain this goal of making the sampled distribution SO(3)-invariant (at least approximately): 1) learning an SO(3)-equivariant denoiser D or 2) learning with rotational augmentation.

Furthermore, to enforce this rotational symmetry, it is common (Xu et al., 2022; Abramson et al., 2024; Wohlwend et al., 2024; Daigavane et al., 2025; Klein et al., 2023b; Dunn & Koes, 2025) to perform an alignment step (either between y and x, or between $D(y;\sigma)$ and x) with the Kabsch-Umeyama algorithms (Kabsch, 1976; Umeyama, 1991) before computing the loss of denoising. However, not much is known about the effect of this alignment step. In particular, does alignment introduce bias in the learning objective? If so, can we improve the alignment operation to reduce this bias? Our paper answers these key questions, and is organized as follows:

- In Section 3, we derive the optimal denoiser for point cloud diffusion. Importantly this denoiser separates into an expectation of the optimal augmented single sample denoiser.
- In Section 4, we show that training a diffusion model is equivalent to matching the single sample optimal denoiser, motivating the construction of better estimators of the optimal denoiser.
- In Section 6, we show the optimal single sample denoiser involves an expectation of a matrix Fisher distribution over SO(3) and rotation alignment corresponds to a zeroth order approximation using the mode of this distribution.
- In Section 7, we build on this insight to obtain better estimators of the optimal denoiser by approximating the expectation via Laplace's method. These estimators enjoy reduced bias relative to the standard alignment based estimator, at *no additional computational cost*, with numerical evidence in Section 8.
- In Section 9, we experiment with these improved estimators to train better diffusion models. At lower noise levels, the effective improvement from using these higher-order correction terms is minimal, suggesting that alignment is already a good enough approximation.

2 PROBLEM SETUP

Point Clouds: Let $x \in \mathbb{R}^{N \times 3}$ represent a point cloud with N points living in 3D space. The entries in x denote the Cartesian coordinates of each point in the point cloud; each row x_i^{\top} is the vector of 3D coordinates of the ith point. We define $\|x\|^2 \equiv \sum_{i=1}^N \|x_i\|^2$.

Often, the point clouds are associated with some SO(3)-invariant features (eg. atomic numbers or charges for atoms in a molecule). These features may be sampled a priori and provided to the denoiser, or undergo their own denoising process with a separate denoiser model (Hoogeboom et al., 2022; Yim et al., 2023; 2024; Campbell et al., 2024). Our analysis is not affected in either case, so we omit these features from further discussion.

Rotations: SO(3) refers to the group of rotations in three dimensions. Since we are working with point clouds which are sets of vectors, it is natural to consider the representation of rotations as rotation matrices $\mathbf{R} \in \mathbb{R}^{3\times 3}$. Thus, the action of a rotation \mathbf{R} on the point cloud $x = [x_i^\top]_{i=1}^N$ is $\mathbf{R} \circ x$ obtained by rotating the coordinates of each point by \mathbf{R} independently:

$$\mathbf{R} \circ x \equiv x \mathbf{R}^{\top} \equiv [x_i^{\top} \mathbf{R}^{\top}]_{i=1}^{N}. \tag{3}$$

Note that rotation matrices are orthonormal: $\mathbf{R}^{\top}\mathbf{R} = \mathbb{I}_3$. Further, the group action is associative:

$$\mathbf{R}_1 \mathbf{R}_2 \circ x = \mathbf{R}_1 \circ (\mathbf{R}_2 \circ x). \tag{4}$$

SO(3)-Invariance: Let p be a distribution over $\mathbb{R}^{N\times 3}$. We say that p is SO(3)-invariant if:

$$p(\mathbf{R} \circ x) = p(x)$$
 for all $\mathbf{R} \in SO(3), x \in \mathbb{R}^{N \times 3}$. (5)

Since there is no way to appropriately normalize a translation-invariant p_x , we center point clouds x such that $\sum_{i=1}^{N} x_i = \vec{0}$, as is commonly done in the literature. This operation does not change our analysis.

Rotational Augmentation: The simple (yet approximate) approach to obtain an equivariant distribution is to augment the data distribution p_x with randomly sampled rotations. In particular, we sample $x \sim p_x$ from our data distribution p_x , $\mathbf{R} \sim u_{\mathbf{R}}$ from the uniform distribution $u_{\mathbf{R}}$ over SO(3) as defined by the Haar measure, and return $\mathbf{R} \circ x \sim \operatorname{Aug}[p_x]$, which is defined as:

$$\operatorname{Aug}[p_x](x') = \int_{SO(3)} p_x(\mathbf{R}^{-1} \circ x') u_{\mathbf{R}}(\mathbf{R}) d\mathbf{R}.$$
 (6)

By construction, $\operatorname{Aug}[p_x](\mathbf{R} \circ x) = p_x(x)u_{\mathbf{R}}(\mathbf{R})$ for any \mathbf{R} . A simple proof (Appendix A.2) shows that $\operatorname{Aug}[p_x]$ is always SO(3)-invariant. When training with rotational augmentation, the loss becomes:

$$\min_{D} l_{\text{aug}}(D) = \min_{D} \mathbb{E}_{\mathbf{R} \sim u_{\mathbf{R}}} \mathbb{E}_{x \sim p_{x}} \mathbb{E}_{\eta \sim p_{\eta}} \mathbb{E}_{\sigma \sim p_{\sigma}} [\|D(\mathbf{R} \circ (x + \sigma \eta); \sigma) - \mathbf{R} \circ x\|^{2}].$$
 (7)

SO(3)-Equivariant Denoisers: An SO(3)-equivariant denoiser D commutes with all rotations \mathbf{R} . Formally:

$$D(\mathbf{R} \circ (x + \sigma \eta)) = \mathbf{R} \circ D(x + \sigma \eta) \tag{8}$$

for all point clouds x, noise η , noise levels σ and rotations **R**.

In Appendix A.1, we show that, given a SO(3)-invariant initial distribution, the result of diffusion sampling with a SO(3)-equivariant denoiser is a SO(3)-invariant distribution. In our case, our initial noise distribution is an isotropic multivariate Gaussian, so the conditions are satisfied. Further, for an equivariant denoiser, data augmentation has no effect (Appendix A.3): $l_{\rm aug}(D) = l_{\rm denoise}(D)$ for an equivariant D.

In Appendix B.1, we show that there is no perfect denoiser under rotational augmentation, implying that $l_{\rm aug}$ has a non-zero minimum. To summarize, the fundamental issue is that there is an ambiguity with respect to which orientation $\mathbf{R} \circ x$ to denoise to. This inspires the idea of alignment to simply cancel out the effect of any such rotation. However, to analyze the alignment step, we first need to characterize the form of the optimal denoiser D^* which minimizes $l_{\rm aug}$.

¹We could have also denoted the augmentated input to D as $\mathbf{R} \circ x + \sigma \eta$, which is equivalent in expectation due to the isotropy of the Gaussian distribution.

3 THE OPTIMAL DENOISER

Having established that there does not exist a perfect denoiser, we can now ask about the optimal denoiser D^* obtaining the minimum possible loss $l_{\text{aug}}(D^*) = \min_D l_{\text{aug}}(D) > 0$. Here, we adapt the derivation performed in Karras et al. (2022).

3.1 THE OPTIMAL DENOISER IN THE SINGLE SAMPLE SETTING

We first state the optimal denoiser D^* in the single sample case, where $p_x(x) = \delta(x - x_0)$. Let $D^*(y; x_0, \sigma)$ be the optimal denoiser for y conditional on a particular x_0 at a noise level σ , which we term the *optimal conditional denoiser*. Then:

$$D^{*}(y; x_{0}, \sigma) = \frac{\mathbb{E}_{\mathbf{R} \sim u_{\mathbf{R}}}[\mathcal{N}(y; \mathbf{R} \circ x_{0}, \sigma^{2} \mathbb{I}_{N \times 3}) \mathbf{R} \circ x_{0}]}{\mathbb{E}_{\mathbf{R} \sim u_{\mathbf{R}}}[\mathcal{N}(y; \mathbf{R} \circ x_{0}, \sigma^{2} \mathbb{I}_{N \times 3})]} = \mathbb{E}_{\mathbf{R} \sim p(\mathbf{R} \mid y, x_{0}, \sigma)}[\mathbf{R} \circ x_{0}]$$
(9)

as we prove in Appendix B.2. Above:

$$p(\mathbf{R} \mid y, x_0, \sigma) = \frac{\mathcal{N}(y; \mathbf{R} \circ x_0, \sigma^2 \mathbb{I}_{N \times 3}) u_{\mathbf{R}}(\mathbf{R})}{\int_{SO(3)} \mathcal{N}(y; \mathbf{R}' x_0, \sigma^2 \mathbb{I}_{N \times 3}) u_{\mathbf{R}}(\mathbf{R}') d\mathbf{R}'}$$
(10)

Thus, we see that the optimal conditional denoiser essentially corresponds to an expectation over different orientations $\mathbf{R} \circ x$. Importantly, it turns out that the optimal conditional denoiser is SO(3)-equivariant:

$$D^*(\mathbf{R} \circ y; x_0, \sigma) = \mathbf{R} \circ D^*(y; x_0, \sigma)$$
(11)

We provide a short proof using the invariance of the Haar measure in Appendix B.5. Further, the optimal conditional denoiser is invariant under rotations \mathbf{R}_{aug} of the conditioning x:

$$D^*(y; \mathbf{R}_{\text{aug}} x, \sigma) = \mathbb{E}_{\mathbf{R} \sim p(\mathbf{R} \mid y, \mathbf{R}_{\text{aug}} \circ x; \sigma)} [\mathbf{R} \circ (\mathbf{R}_{\text{aug}} \circ x)] = D^*(y; x, \sigma)$$
(12)

3.2 THE OPTIMAL DENOISER IN THE GENERAL SETTING

In the general setting where p_x is arbitrary, the optimal denoiser $D^*(y; \sigma)$ is an expectation over $x \sim p(x \mid y, \sigma)$ of the optimal conditional denoiser $D^*(y; x, \sigma)$, as we prove in Appendix B.3:

$$D^{*}(y;\sigma) = \mathbb{E}_{x,\mathbf{R} \sim p(x,\mathbf{R} \mid y,\sigma)}[\mathbf{R} \circ x]$$

$$= \mathbb{E}_{x \sim p(x \mid y,\sigma)} \mathbb{E}_{\mathbf{R} \sim p(\mathbf{R} \mid y,x,\sigma)}[\mathbf{R} \circ x] = \mathbb{E}_{x \sim p(x \mid y,\sigma)}[D^{*}(y;x,\sigma)]$$
(13)

It follows from the SO(3)-equivariance of $D^*(y; x, \sigma)$ that $D^*(y; \sigma)$ is also SO(3)-equivariant.

Given that there is an analytic expression of the optimal denoiser, a natural question arises. Instead of minimizing the usual denoising loss (Equation 1), can we instead try to match the optimal denoiser? Indeed, we shall see that these approaches are actually identical.

4 MATCHING THE OPTIMAL DENOISER

Here, we motivate why we would want to match the optimal denoiser D^* . To do so, we first consider matching to some general estimator $D_{\rm est}(y;x,{\bf R},\sigma)$ potentially dependent on all the random variables. Given any estimator $D_{\rm est}(y;x,{\bf R},\sigma)$ we want to match to D, we can define a matching loss by:

$$l_{\text{est}}(D; D_{\text{est}}) = \mathbb{E}_{\mathbf{R} \sim u_{\mathbf{R}}} \mathbb{E}_{x \sim p_{x}} \mathbb{E}_{\eta \sim p_{\eta}} \mathbb{E}_{\sigma \sim p_{\sigma}} [\|D(\mathbf{R} \circ (x + \sigma \eta); \sigma) - D_{\text{est}}(\mathbf{R} \circ (x + \sigma \eta); x, \mathbf{R}, \sigma)\|^{2}]$$

$$= \mathbb{E}_{\mathbf{R} \sim u_{\mathbf{R}}} \mathbb{E}_{x \sim p_{x}} \mathbb{E}_{\sigma \sim p_{\sigma}} \mathbb{E}_{y \sim p(y|x,\sigma,\mathbf{R})} [\|D(y;\sigma) - D_{\text{est}}(y; x, \mathbf{R}, \sigma)\|^{2}]$$

$$= \mathbb{E}_{\sigma \sim p_{\sigma}} \mathbb{E}_{y \sim p(y|\sigma)} \mathbb{E}_{x \sim p(x \mid y,\sigma)} \mathbb{E}_{\mathbf{R} \sim p(\mathbf{R} \mid y,x,\sigma)} [\|D(y;\sigma) - D_{\text{est}}(y; x, \mathbf{R}, \sigma)\|^{2}]$$
(14)

after identifying $y \equiv \mathbf{R} \circ (x + \sigma \eta)$. As we prove in Appendix B.7, averaging an estimator D_{est} over $\mathbf{R} \sim p(\mathbf{R} \mid y, x, \sigma)$ to obtain a new estimator $\mathbb{E}_{\mathbf{R} \sim p(\mathbf{R} \mid y, x, \sigma)}[D_{\text{est}}]$ gives us an equivalent loss from a minimization perspective: $l_{\text{est}}(D; \mathbb{E}_{\mathbf{R} \sim p(\mathbf{R} \mid y, x, \sigma)}[D_{\text{est}}]) = l_{\text{est}}(D; D_{\text{est}}) + C$, where C is a constant that does not depend on D. The same reasoning applies to averaging an estimator D_{est} over $x \sim p(x \mid y, \sigma)$ to obtain a new estimator $\mathbb{E}_{x \sim p(x \mid y, \sigma)}[D_{\text{est}}]$.

Setting $D_{\rm est}(y;x,\mathbf{R},\sigma) \equiv \mathbf{R} \circ x$ recovers $l_{\rm aug}$. Now, for this choice of $D_{\rm est}$, $\mathbb{E}_{\mathbf{R} \sim p(\mathbf{R} \mid y,x,\sigma)}[D_{\rm est}]$ corresponds to the *optimal conditional denoiser*. Further, $\mathbb{E}_{x \sim p(x \mid y,\sigma)}\mathbb{E}_{\mathbf{R} \sim p(\mathbf{R} \mid y,x,\sigma)}[D_{\rm est}]$ corresponds to the *optimal denoiser*. Thus, from the previous arguments, optimal denoiser matching is *equivalent* to the standard denoising loss.

The advantage of averaging, however, comes from a practical perspective. In practice, we can only estimate this loss through sampling which introduces a sampling error for each random variable (ie, \mathbf{x}, \mathbf{R}) in the argument. By averaging, we remove the dependence of the argument on the random variable being averaged over and reduce this sampling error.

Performing the averaging over x is tricky, because the expectation over $p(x \mid y, \sigma)$ requires access to p_x . Approximating this expectation over a finite set of x can suffer from overfitting (Vastola, 2025; Kadkhodaie et al., 2024; Li et al., 2023). Niedoba et al. (2024) tried to address this by building estimators based on the nearest-neighbor approximation. However, the averaging over \mathbf{R} to give the optimal conditional denoiser is indeed feasible, as we discuss next.

In conclusion, rather than optimizing l_{aug} , we can instead match to the optimal conditional denoiser:

$$l_{\text{est}}(D; D^*(y, x, \sigma)) = l_{\text{match}}(D) = \mathbb{E}_{\sigma \sim p_{\sigma}} \mathbb{E}_{y \sim p(y|\sigma)} \mathbb{E}_{x \sim p(x|y, \sigma)} [\|D(y; \sigma) - D^*(y; x, \sigma)\|^2].$$

$$(15)$$

5 THE MATRIX FISHER DISTRIBUTION ON SO(3)

Here, we connect the optimal conditional denoiser to the matrix Fisher distribution. Recall our expression of $D^*(y; x, \sigma)$ involves an expectation over $p(\mathbf{R} \mid y, x, \sigma)$. Some simple algebraic manipulation (Appendix B.4) shows us that:

$$p(\mathbf{R} \mid y, x, \sigma) \propto \exp\left(-\frac{\|y - \mathbf{R} \circ x\|^2}{2\sigma^2}\right) \propto \exp\left(\operatorname{Tr}\left[\frac{y^{\top} x}{2\sigma^2} \mathbf{R}\right]\right)$$
 (16)

In particular, the distribution $p(\mathbf{R} \mid y, x, \sigma)$ belongs to a well-studied family of distributions called the matrix Fisher distribution over SO(3) (Mohlin et al., 2020; Lee, 2018). This distribution is parametrized by a 3×3 matrix F:

$$MF(\mathbf{R}; F) = \frac{\exp \text{Tr}[F^{\top}\mathbf{R}]}{Z(F)}$$
(17)

where Z(F) is the partition function, ensuring that the distribution is normalized over SO(3). Thus, conditional on y, x and σ , \mathbf{R} is distributed according to a matrix Fisher distribution with $F = \frac{y^{\top}x}{\sigma^2} \in \mathbb{R}^{3\times 3}$. We can write:

$$D^*(y; x, \sigma) = \mathbb{E}_{\mathbf{R} \sim \mathrm{MF}\left(\mathbf{R}; \frac{y^{\top} x}{\sigma^2}\right)}[\mathbf{R} \circ x] = \mathbb{E}_{\mathbf{R} \sim \mathrm{MF}\left(\mathbf{R}; \frac{y^{\top} x}{\sigma^2}\right)}[\mathbf{R}] \circ x.$$
(18)

Therefore computing the optimal denoiser involves computing the first moment of a matrix Fisher distribution.

6 ROTATIONAL ALIGNMENT

It turns out rotation alignment gives a very good approximation for the first moment. Assuming x, y have no rotational self symmetries (which is generically the case), then $\mathrm{MF}\left(\mathbf{R}; \frac{y^{\top}x}{\sigma^2}\right)$ is a unimodal distribution. In fact, for small σ this distribution becomes very sharply peaked, so the mode becomes a good approximation of the first moment.

We can see the mode of the distribution satisfies:

$$\mathbf{R}_{\text{mode}} = \underset{\mathbf{R} \in SO(3)}{\operatorname{argmax}} \operatorname{MF} \left(\mathbf{R}; \frac{y^{\top} x}{\sigma^{2}} \right) = \underset{\mathbf{R} \in SO(3)}{\operatorname{argmax}} \operatorname{Tr} \left[\frac{y^{\top} x}{2\sigma^{2}} \mathbf{R} \right] = \underset{\mathbf{R} \in SO(3)}{\operatorname{argmin}} - \operatorname{Tr}[y^{\top} x \mathbf{R}]$$

$$= \underset{\mathbf{R} \in SO(3)}{\operatorname{argmin}} \frac{1}{2} (\operatorname{Tr}[y^{\top} y] - 2 \operatorname{Tr}[y^{\top} x \mathbf{R}] + \operatorname{Tr}[\mathbf{R}^{\top} x^{\top} x \mathbf{R}) = \underset{\mathbf{R} \in SO(3)}{\operatorname{argmin}} ||y - \mathbf{R} \circ x||^{2} \quad (19)$$

$$= \mathbf{R}^{*}(y, x) \quad (20)$$

where $\mathbf{R}^*(y,x)$ is the optimal rotation for aligning x to y, exactly the rotation matrix returned by the Kabsch and Proscrutes alignment algorithms.

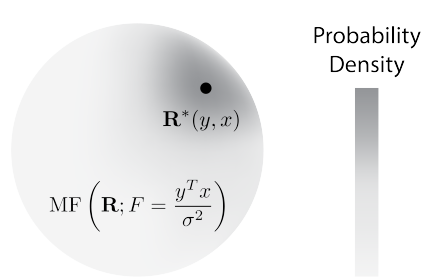


Figure 2: A depiction of the unimodal MF(\mathbf{R} ; F) over SO(3), highlighting the mode $\mathbf{R}^*(y, x)$. As σ decreases, the distribution becomes more peaked around $\mathbf{R}^*(y, x)$.

This marks our first insight: alignment allows us to approximate $\mathbb{E}_{\mathbf{R}}[\mathbf{R}] \approx \mathbf{R}^*(y,x)$ in the optimal single sample denoiser (Equation 9) so

$$D^*(y; x, \sigma) = \mathbb{E}_{\mathbf{R}}[\mathbf{R}] \circ x \approx \mathbf{R}^*(y, x)x.$$

Substituting $\mathbf{R}^*(y,x)x$ for D_{est} in Equation 14, we obtain

$$l_{\text{align-aug}}(D) = \mathbb{E}_{\mathbf{R} \sim u_{\mathbf{R}}} \mathbb{E}_{x \sim p_{x}} \mathbb{E}_{\eta \sim p_{\eta}} \mathbb{E}_{\sigma \sim p_{\sigma}} [\|D(\mathbf{R} \circ (x + \sigma \eta); \sigma) - \mathbf{R}^{*}(y, x) \circ x\|^{2}]$$
(21)

exactly the loss used for rotation alignment!

Can better estimators for D^* be constructed by better approximations of $\mathbb{E}_{\mathbf{R}}[\mathbf{R}]$? Yes! In Section 7, we show that there exist better approximators of $\mathbb{E}_{\mathbf{R}}[\mathbf{R}]$ with no additional asymptotic runtime cost over alignment.

7 APPROXIMATING THE OPTIMAL DENOISER VIA AN ASYMPTOTIC EXPANSION OF THE MATRIX-FISHER DISTRIBUTION

Here, we derive additional correction terms to the moment $\mathbb{E}_{\mathbf{R}}[\mathbf{R}]$ in the limit of $\sigma \to 0$. These correction terms can be implemented with no additional cost.

7.1 FOR A GENERAL MATRIX FISHER DISTRIBUTION

We provide a high level summary of the method used to derive additional correction terms. More detail can be found in Appendix C.

We note that the partition function $Z(F) = \int_{SO(3)} \exp(\text{Tr}[F^{\top}\mathbf{R}]) d\mathbf{R}$ gives all the information we need. In particular, taking derivatives of Z(F) allows us to calculate any necessary moments. For example,

$$\mathbb{E}_{\mathbf{R} \sim \mathrm{MF}(\mathbf{R};F)}[\mathbf{R}] = \frac{\int_{SO(3)} \mathbf{R} \exp(\mathrm{Tr}[F^{\top}\mathbf{R}]) d\mathbf{R}}{Z(F)} = \frac{\frac{d}{dF} Z(F)}{Z(F)} = \frac{d}{dF} \ln Z(F)$$
(22)

using the trace derivative identity: $\frac{d}{dF} \operatorname{Tr}[F^{\top} \mathbf{R}] = \mathbf{R}$. To control peakedness, we replace F with λF so that as $\lambda \to \infty$, the distribution becomes a delta function centered at the mode.

Next, recall that in Kabsch alignment we use SVD to decompose where $U, V \in SO(3)$ and $S = \operatorname{diag}[s_1, s_2, s_3]$ where $s_1 \geq s_2 \geq |s_3|$. It turns out that $Z(\lambda F) = Z(\lambda S)$ so we restrict to only expanding Z for diagonal S. To approximate $Z(\lambda S)$, we use Laplace's method.

First, we choose to use the exponential map parameterization $\mathbf{R}(\theta_x, \theta_y, \theta_z) = \exp(\theta_x R_x + \theta_y R_y + \theta_z R_z)$. Next, we Taylor expand the argument $\text{Tr}[S^{\top}\mathbf{R}(\boldsymbol{\theta})]$ around $\boldsymbol{\theta} = 0$. It is not hard to check that \mathbb{I} maximizes this so there is no first order term. Hence taking up to second order terms, we obtain some $\exp(\lambda A_0(S) + \lambda \boldsymbol{\theta}^{\top} A_2(S)\boldsymbol{\theta})$ which can be interpreted as a Gaussian because A_2 must be negative

definite since \mathbb{I} is the maximum. In some sense this captures the peak of the distribution and we can write

$$\exp(\operatorname{Tr}[\lambda S^{\top} \mathbf{R}(\boldsymbol{\theta})]) = \exp(\lambda A_0(S) + \lambda \boldsymbol{\theta}^{\top} A_2(S)\boldsymbol{\theta}) B(\boldsymbol{\theta}, S, \lambda)$$

Next, we can perform the usual Taylor expansion of $B(\theta,S,\lambda)\mu(\theta)$, the remaining terms in the integral where $\mu(\theta)$ is the corresponding Haar measure. We also do this around $\theta=0$ because only the neighborhood around the peak matters. Finally, we note that as $\lambda\to\infty$, the width of the peak described by $\exp(\lambda A_0(S) + \lambda \theta^\top A_2(S)\theta)$ decreases. Hence, replacing the domain $\{|\theta| < \pi\}$ with the larger domain $\{\theta \in \mathbb{R}^3\}$ not gives us a good approximation for each of the expanded terms, but also gives us Gaussian integrals which are analytically evaluable.

Finally, we obtain an expression of the form:

$$Z(\lambda S) = N(S, \lambda) \left(1 + L_1(S) \frac{1}{\lambda} + L_2(S) \frac{1}{\lambda^2} + L_3(S) \frac{1}{\lambda^3} + \dots \right)$$
 (23)

where $N(S, \lambda)$ is a normalization term. The corresponding expected rotation can be computed as:

$$\mathbb{E}_{\mathbf{R} \sim \mathrm{MF}(\mathbf{R}; \lambda S)}[\mathbf{R}] = \frac{1}{\lambda} \operatorname{diag} \left[\frac{\partial \ln Z(\lambda S)}{\partial s_1}, \frac{\partial \ln Z(\lambda S)}{\partial s_1}, \frac{\partial \ln Z(\lambda S)}{\partial s_3} \right]$$

$$= \mathbb{I} + C_1(S) \frac{1}{\lambda} + C_2(S) \frac{1}{\lambda^2} + \dots$$
(24)

For an arbitrary $F' = USV^{\top}$, we would then have:

$$\mathbb{E}_{\mathbf{R} \sim \mathrm{MF}(\mathbf{R}; \lambda F')}[\mathbf{R}] = U \mathbb{E}_{\mathbf{R} \sim \mathrm{MF}(\mathbf{R}; \lambda S)}[\mathbf{R}] V^{\top}.$$
 (25)

7.2 FOR THE SPECIFIC $F = \frac{y^{\top}x}{\sigma^2}$

We are specifically interested in the case where $F = \frac{y^\top x}{\sigma^2}$, as $p(\mathbf{R} \mid y, x, \sigma) = \mathrm{MF}(\mathbf{R}; \frac{y^\top x}{\sigma^2})$. From the Kabsch algorithm, we have that $\mathbf{R}^*(y, x) = UV^\top$ where $U, S, V^\top = \mathrm{SVD}(y^\top x) = \mathrm{SVD}(F')$ with $\det(U) = \det(V) = 1$ and $S = \operatorname{diag}[s_1, s_2, s_3]$ where $s_1 \geq s_2 \geq |s_3|$.

Following the procedure outlined in Section 7, we used Mathematica (Inc.) to find the coefficients in Equation 24 explicitly:

$$C_1(S) = -\frac{1}{2}\operatorname{diag}\left[\frac{1}{s_1 + s_2} + \frac{1}{s_1 + s_3}, \frac{1}{s_2 + s_1} + \frac{1}{s_2 + s_3}, \frac{1}{s_3 + s_1} + \frac{1}{s_3 + s_2}\right]$$

$$C_2(S) = -\frac{1}{8}\operatorname{diag}\left[\frac{1}{(s_1 + s_2)^2} + \frac{1}{(s_1 + s_3)^2}, \frac{1}{(s_2 + s_1)^2} + \frac{1}{(s_2 + s_3)^2}, \frac{1}{(s_3 + s_1)^2} + \frac{1}{(s_3 + s_2)^2}\right]$$

$$(26)$$

These represent the first-order and second-order correction terms respectively. This approximation is exact in the limit $\sigma \to 0$.

Equation 24 allows us to approximate the optimal conditional denoiser as:

$$D^*(y;x) = \mathbb{E}_{\mathbf{R} \sim p(\mathbf{R} \mid y, x, \sigma)}[\mathbf{R} \circ x] = \mathbb{E}_{\mathbf{R} \sim p(\mathbf{R} \mid y, x, \sigma)}[\mathbf{R}] \circ x \tag{28}$$

$$= (\mathbf{R}^*(y, x) + \sigma^2 B_1(y, x) + \sigma^4 B_2(y, x)) \circ x + \mathcal{O}(\sigma^5).$$
 (29)

where $B_1(y,x) = UC_1(S)V^{\top}$ and $B_2(y,x) = UC_2(S)V^{\top}$.

Thus, alignment corresponds to the *zeroth-order* (in σ) approximation of $D^*(y; x, \sigma)$. From Equation 29, we define the successive *first-order* and *second-order* approximations to the optimal denoiser:

$$D_0^*(y; x, \sigma) = \mathbf{R}^*(y, x) \circ x \tag{30}$$

$$D_1^*(y; x, \sigma) = (\mathbf{R}^*(y, x) + \sigma^2 B_1(y, x)) \circ x \tag{31}$$

$$D_2^*(y; x, \sigma) = (\mathbf{R}^*(y, x) + \sigma^2 B_1(y, x) + \sigma^4 B_2(y, x)) \circ x \tag{32}$$

Our improved estimators D_1^* and D_2^* have reduced bias relative to the usual alignment-based D_0^* . Importantly, these improved estimators can be constructed at no additional computational cost to the standard Kabsch alignment, since U and V have already been computed. They simply correspond to adjusting the rotation \mathbf{R}^* before multiplying with x.

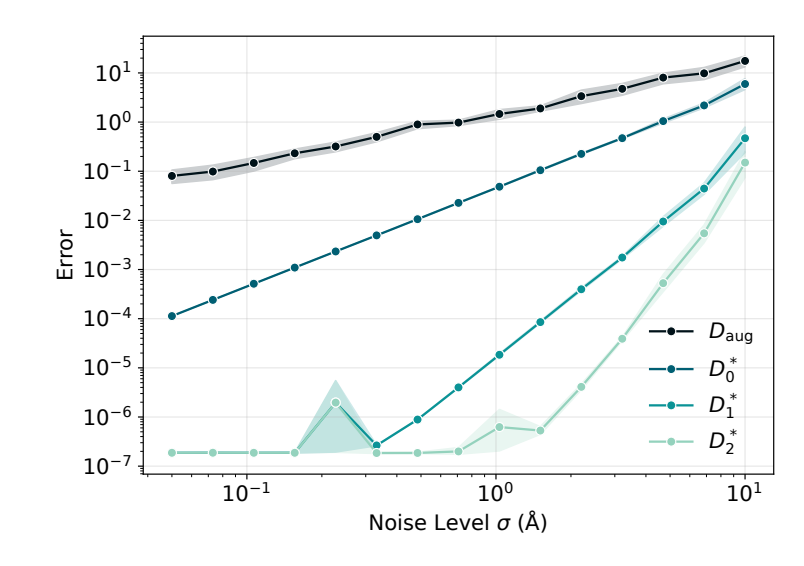


Figure 3: Mean-squared error relative to the optimal denoiser $D^*(y;x)$ as a function of σ . x here is a randomly chosen conformation of the AEQN tetrapeptide from the TIMEWARP 4AA-LARGE dataset, and y is sampled as $x + \sigma \eta$. For larger σ , we see that the error rates drop significantly using higher order correction terms. For smaller σ , we quickly reach the regime where error is dominated by numerical precision rather than approximation error when using higher order correction terms.

8 NUMERICAL ERROR IN APPROXIMATIONS OF THE OPTIMAL DENOISER

In Figure 3, we compute error in the zeroth-order D_0^* , first-order D_1^* , and second-order D_2^* approximations compared to an estimate of $D^*(y;x)$ obtained by numerically integrating the expectation in Equation 28 in Mathematica, which automatically adjusts the resolution of the grid for the numerical quadrature on SO(3).

In the next section, we experiment with the practical utility of these estimators.

9 RESULTS IN PRACTICE

We train a simple 2-layer MLP (with 2.3M parameters) on 3D configurations of the tetrapeptide AEQN as obtained from the TIMEWARP 4AA-LARGE dataset (Klein et al., 2023a), utilizing the codebase of the JAMUN (Daigavane et al., 2025) model. We train this model using the losses corresponding to the estimators $D_{\rm aug}, D_0^*, D_1^*$ and D_2^* discussed above, at 4 different noise levels $\sigma=0.5\,\text{Å},\ 1.0\,\text{Å},\ 5\,\text{Å}$ and $10\,\text{Å}$. This captures most of the noise levels usually used to train diffusion models on data of this size (Wohlwend et al., 2024). We perform two experiments which allow us to measure the impact of the estimators in learning 1. the optimal denoiser and 2. the optimal conditional denoiser.

- 1. We sample x from all 50000 frames of a molecular dynamics simulation for the AEQN peptide, as obtained from Klein et al. (2023a).
- 2. We fix x as the first frame of the same molecular dynamics simulation.

The results are shown in Figure 4 and Figure 5, where we report the RMSD (root mean square deviation) to the ground truth x. In Appendix D, we also show plots of the aligned RMSD for the same training runs.

We see that at the largest noise level, the second-order correction tends to diverge. At the lowest noise levels, the magnitude of the correction is not significant, and all estimators perform similarly. We see that in practice, the zeroth-order approximation D_0^* is usually good enough at the important noise levels; in particular, it seems like the model is unable to take advantage of the variance reduction from the higher-order corrections. We hypothesize that this may be due to the fact that the variance of the

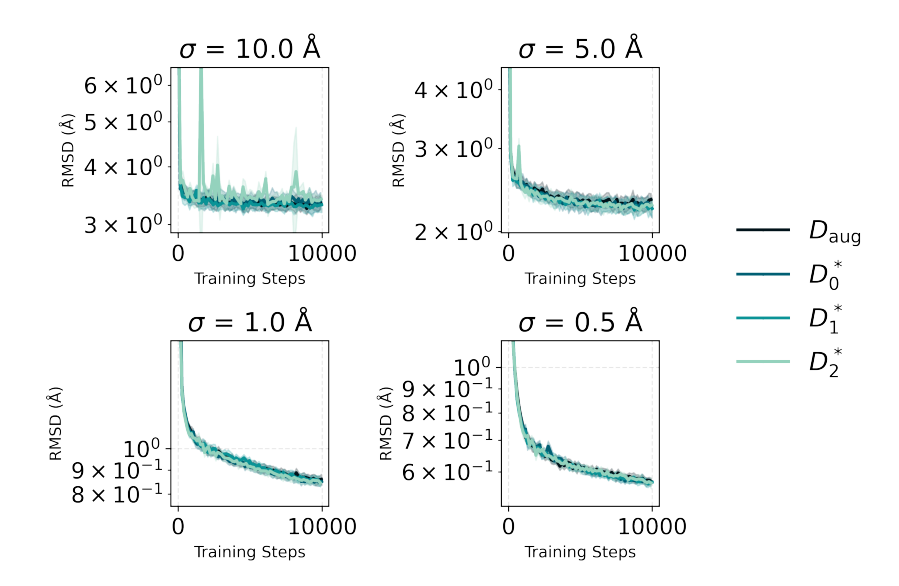


Figure 4: Training progress for the MLP, as measured by RMSD to ground-truth x (sampled from all frames), when trained using D_{aug} , D_0^* , D_1^* and D_2^* .

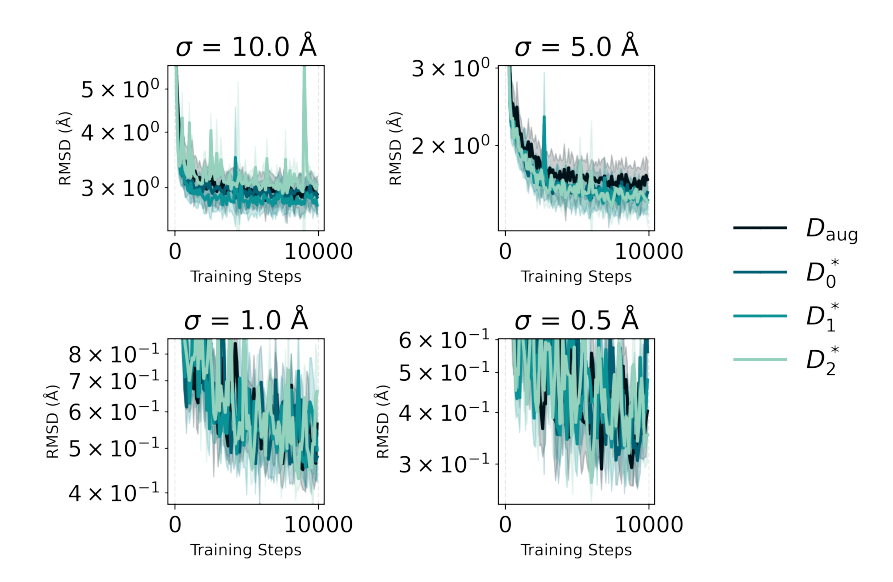


Figure 5: Training progress for the MLP, as measured by RMSD to ground-truth x (fixed as the first frame), when trained using D_{aug} , D_0^* , D_1^* and D_2^* .

gradients over the multiple x is much greater than the variance of the gradients due to the rotational symmetries. These results are preliminary, but they suggest that alignment itself may not be super critical to learn a good denoiser.

10 ETHICS STATEMENT

We have read and agree to comply to the ICLR Code of Ethics. Our results are primarily theoretical and specific to the field of computational biology; we do not anticipate any negative impacts on society from this research.

11 REPRODUCIBILITY STATEMENT

We have provided the Mathematica notebooks, our training code, and data (obtained from the TIMEWARP dataset, with the authors' permission) to reproduce all of our results as supplementary material.

REFERENCES

- Josh Abramson, Jonas Adler, Jack Dunger, Richard Evans, Tim Green, Alexander Pritzel, Olaf Ronneberger, Lindsay Willmore, Andrew J. Ballard, Joshua Bambrick, Sebastian W. Bodenstein, David A. Evans, Chia-Chun Hung, Michael O'Neill, David Reiman, Kathryn Tunyasuvunakool, Zachary Wu, Akvilė Žemgulytė, Eirini Arvaniti, Charles Beattie, Ottavia Bertolli, Alex Bridgland, Alexey Cherepanov, Miles Congreve, Alexander I. Cowen-Rivers, Andrew Cowie, Michael Figurnov, Fabian B. Fuchs, Hannah Gladman, Rishub Jain, Yousuf A. Khan, Caroline M. R. Low, Kuba Perlin, Anna Potapenko, Pascal Savy, Sukhdeep Singh, Adrian Stecula, Ashok Thillaisundaram, Catherine Tong, Sergei Yakneen, Ellen D. Zhong, Michal Zielinski, Augustin Žídek, Victor Bapst, Pushmeet Kohli, Max Jaderberg, Demis Hassabis, and John M. Jumper. Accurate structure prediction of biomolecular interactions with AlphaFold 3. *Nature*, 630(8016):493–500, Jun 2024. ISSN 1476-4687. doi: 10.1038/s41586-024-07487-w. URL https://doi.org/10.1038/s41586-024-07487-w.
- Andrew Campbell, Jason Yim, Regina Barzilay, Tom Rainforth, and Tommi Jaakkola. Generative flows on discrete state-spaces: Enabling multimodal flows with applications to protein co-design, 2024. URL https://arxiv.org/abs/2402.04997.
- Ameya Daigavane, Bodhi P. Vani, Darcy Davidson, Saeed Saremi, Joshua Rackers, and Joseph Kleinhenz. Jamun: Bridging smoothed molecular dynamics and score-based learning for conformational ensembles, 2025. URL https://arxiv.org/abs/2410.14621.
- Ian Dunn and David R. Koes. Flowmol3: Flow matching for 3d de novo small-molecule generation, 2025. URL https://arxiv.org/abs/2508.12629.
- Emiel Hoogeboom, Victor Garcia Satorras, Clément Vignac, and Max Welling. Equivariant diffusion for molecule generation in 3d, 2022. URL https://arxiv.org/abs/2203.17003.
- Wolfram Research, Inc. Mathematica, Version 14.2. URL https://www.wolfram.com/mathematica.Champaign, IL, 2024.
- W. Kabsch. A solution for the best rotation to relate two sets of vectors. *Acta Crystallographica Section A*, 32(5):922–923, Sep 1976. doi: 10.1107/S0567739476001873. URL https://doi.org/10.1107/S0567739476001873.
- Zahra Kadkhodaie, Florentin Guth, Eero P Simoncelli, and Stéphane Mallat. Generalization in diffusion models arises from geometry-adaptive harmonic representations. In *The Twelfth International Conference on Learning Representations*, 2024. URL https://openreview.net/forum?id=ANvmVS2Yr0.
- Tero Karras, Miika Aittala, Timo Aila, and Samuli Laine. Elucidating the design space of diffusion-based generative models, 2022.
- Leon Klein, Andrew Y. K. Foong, Tor Erlend Fjelde, Bruno Mlodozeniec, Marc Brockschmidt, Sebastian Nowozin, Frank Noé, and Ryota Tomioka. Timewarp: Transferable acceleration of molecular dynamics by learning time-coarsened dynamics, 2023a. URL https://arxiv.org/abs/2302.01170.

- Leon Klein, Andreas Krämer, and Frank Noe. Equivariant flow matching. In *Thirty-seventh Conference on Neural Information Processing Systems*, 2023b. URL https://openreview.net/forum?id=eLH2NFOO1B.
 - Taeyoung Lee. Bayesian Attitude Estimation With the Matrix Fisher Distribution on SO(3). *IEEE Transactions on Automatic Control*, 63(10):3377–3392, 2018. doi: 10.1109/TAC.2018.2797162.
 - Puheng Li, Zhong Li, Huishuai Zhang, and Jiang Bian. On the generalization properties of diffusion models. In *Thirty-seventh Conference on Neural Information Processing Systems*, 2023. URL https://openreview.net/forum?id=hCUG1MCFk5.
 - David Mohlin, Josephine Sullivan, and Gérald Bianchi. Probabilistic orientation estimation with matrix fisher distributions. *Advances in Neural Information Processing Systems*, 33:4884–4893, 2020.
 - Matthew Niedoba, Dylan Green, Saeid Naderiparizi, Vasileios Lioutas, Jonathan Wilder Lavington, Xiaoxuan Liang, Yunpeng Liu, Ke Zhang, Setareh Dabiri, Adam Ścibior, Berend Zwartsenberg, and Frank Wood. Nearest neighbour score estimators for diffusion generative models, 2024. URL https://arxiv.org/abs/2402.08018.
 - Jiaming Song, Chenlin Meng, and Stefano Ermon. Denoising diffusion implicit models, 2022. URL https://arxiv.org/abs/2010.02502.
 - S. Umeyama. Least-squares estimation of transformation parameters between two point patterns. *IEEE Transactions on Pattern Analysis and Machine Intelligence*, 13(4):376–380, 1991. doi: 10.1109/34.88573.
 - John J. Vastola. Generalization through variance: how noise shapes inductive biases in diffusion models, 2025. URL https://arxiv.org/abs/2504.12532.
 - Jeremy Wohlwend, Gabriele Corso, Saro Passaro, Mateo Reveiz, Ken Leidal, Wojtek Swiderski, Tally Portnoi, Itamar Chinn, Jacob Silterra, Tommi Jaakkola, and Regina Barzilay. Boltz-1 democratizing biomolecular interaction modeling. *bioRxiv*, 2024. doi: 10.1101/2024.11.19.624167. URL https://www.biorxiv.org/content/early/2024/11/20/2024.11.19.624167.
 - Minkai Xu, Lantao Yu, Yang Song, Chence Shi, Stefano Ermon, and Jian Tang. GeoDiff: a Geometric Diffusion Model for Molecular Conformation Generation, 2022. URL https://arxiv.org/abs/2203.02923.
 - Shuai Yang, Yukang Chen, Luozhou Wang, Shu Liu, and Yingcong Chen. Denoising diffusion step-aware models, 2024. URL https://arxiv.org/abs/2310.03337.
 - Jason Yim, Andrew Campbell, Andrew YK Foong, Michael Gastegger, José Jiménez-Luna, Sarah Lewis, Victor Garcia Satorras, Bastiaan S Veeling, Regina Barzilay, Tommi Jaakkola, et al. Fast protein backbone generation with se (3) flow matching. *arXiv preprint arXiv:2310.05297*, 2023.
 - Jason Yim, Andrew Campbell, Emile Mathieu, Andrew Y. K. Foong, Michael Gastegger, Jose Jimenez-Luna, Sarah Lewis, Victor Garcia Satorras, Bastiaan S. Veeling, Frank Noe, Regina Barzilay, and Tommi Jaakkola. Improved motif-scaffolding with SE(3) flow matching. *Transactions on Machine Learning Research*, 2024. ISSN 2835-8856. URL https://openreview.net/forum?id=falne8xDGn.

PROOFS

EQUIVARIANT DENOISERS SAMPLE INVARIANT DISTRIBUTIONS

The proof is similar to that of Proposition 1 in Xu et al. (2022).

Suppose that $p_u(; \sigma_{i+1})$ is a SO(3)-invariant distribution:

$$p_y(y_{i+1}; \sigma_{i+1}) = p_y(\mathbf{R} \circ y_{i+1}; \sigma_{i+1})$$
(33)

Using the DDIM update rule (Equation 2) at step (i+1), we see that the next distribution $p_u(;\sigma_i)$ is also SO(3)-invariant. Under an arbitrary rotation **R**:

$$DDIM_{i+1}(\mathbf{R} \circ y_{i+1}) = \mathbf{R} \circ y_{i+1} + \left(1 - \frac{\sigma_i}{\sigma_{i+1}}\right) \left(D(\mathbf{R} \circ y_{i+1}, \sigma_{i+1}) - \mathbf{R} \circ y_{i+1}\right)$$
(34)

$$= \mathbf{R} \circ y_{i+1} + \left(1 - \frac{\sigma_i}{\sigma_{i+1}}\right) \left(\mathbf{R} \circ y_{i+1}, \sigma_{i+1}\right) - \mathbf{R} \circ y_{i+1}$$

$$= \mathbf{R} \circ y_{i+1} + \left(1 - \frac{\sigma_i}{\sigma_{i+1}}\right) \left(\mathbf{R} \circ D(y_{i+1}, \sigma_{i+1}) - \mathbf{R} \circ y_{i+1}\right)$$
(35)

$$= \mathbf{R} \circ \left(y_{i+1} + \left(1 - \frac{\sigma_i}{\sigma_{i+1}} \right) \left(D(y_{i+1}, \sigma_{i+1}) - y_{i+1} \right) \right)$$
 (36)

$$= \mathbf{R} \circ y_{i+1} \tag{37}$$

$$= \mathbf{R} \circ y_{i+1}$$

$$= \mathbf{R} \circ \mathrm{DDIM}_{i+1}(y_{i+1})$$
(38)

We used the SO(3)-equivariance of the denoiser above: $D(\mathbf{R} \circ y_{i+1}, \sigma_{i+1}) = \mathbf{R} \circ D(y_{i+1}, \sigma_{i+1})$ for all y_{i+1} .

Hence:

$$p_y(y_i; \sigma_i) = \int p(y_i|y_{i+1}) p_y(y_{i+1}; \sigma_{i+1}) dy_{i+1}$$
(39)

$$= \int \delta(y_i - \text{DDIM}_{i+1}(y_{i+1})) p_y(y_{i+1}; \sigma_{i+1}) dy_{i+1}$$
(40)

$$= \int \delta(y_i - \text{DDIM}_{i+1}(y_{i+1})) p_y(\mathbf{R} \circ y_{i+1}; \sigma_{i+1}) dy_{i+1}$$

$$\tag{41}$$

$$= \int \delta(\mathbf{R} \circ y_i - \mathbf{R} \circ \mathrm{DDIM}_{i+1}(y_{i+1})) p_y(\mathbf{R} \circ y_{i+1}; \sigma_{i+1}) dy_{i+1}$$
(42)

$$= \int \delta(\mathbf{R} \circ y_i - \mathbf{R} \circ \mathrm{DDIM}_{i+1}(y_{i+1})) p_y(\mathbf{R} \circ y_{i+1}; \sigma_{i+1}) dy_{i+1}$$

$$= \int \delta(\mathbf{R} \circ y_i - \mathrm{DDIM}_{i+1}(\mathbf{R} \circ y_{i+1})) p_y(\mathbf{R} \circ y_{i+1}; \sigma_{i+1}) dy_{i+1}$$

$$(42)$$

$$\int \delta(\mathbf{P} \circ g_i - \mathbf{P} \mathbf{P} \mathbf{M}_{i+1} (\mathbf{P} \circ g_{i+1})) p_g(\mathbf{P} \circ g_{i+1}) \otimes g_{i+1}$$
(14)

$$= \int \delta(\mathbf{R} \circ y_i - \mathrm{DDIM}_{i+1}(y'_{i+1})) p_y(y'_{i+1}; \sigma_{i+1}) dy'_{i+1}$$

$$= p_y(\mathbf{R} \circ y_i; \sigma_i)$$

$$\tag{44}$$

(45)

using the change of variables $y'_{i+1} \equiv \mathbf{R} \circ y_{i+1}$ which does not induce any change of measure. Hence,

$$p_y(;\sigma_i)$$

is a SO(3)-invariant distribution. The initial distribution is $\mathcal{N}(0, \sigma_M^2 \mathbb{I}_d)$, which is also SO(3)invariant distribution due to the isotropy of the multivariate Gaussian. We can conclude that at each noise level σ_i in the diffusion process, the $p_y(;\sigma_i)$ is SO(3)-invariant.

The same proof can be generalized to stochastic samplers such as DDSM (Yang et al., 2024).

A.2 ROTATIONALLY AUGMENTED DISTRIBUTIONS ARE INVARIANT

For any arbitrary rotation \mathbf{R} :

$$\operatorname{Aug}[p_x](\mathbf{R} \circ x) = \int_{SO(3)} p_x(\mathbf{R}'^{-1}\mathbf{R} \circ x) u_{\mathbf{R}}(\mathbf{R}') d\mathbf{R}'$$
(46)

$$= \int_{SO(3)} p_x((\mathbf{R}^{-1}\mathbf{R}')^{-1} \circ x) u_{\mathbf{R}}(\mathbf{R}(\mathbf{R}^{-1}\mathbf{R}')) d(\mathbf{R}\mathbf{R}^{-1}\mathbf{R}')$$
(47)

$$= \int_{SO(3)} p_x(\mathbf{R}^{\prime\prime-1} \circ x) u_{\mathbf{R}}(\mathbf{R}\mathbf{R}^{\prime\prime}) d(\mathbf{R}\mathbf{R}^{\prime\prime})$$
(48)

$$= \int_{SO(3)} p_x(\mathbf{R}^{\prime\prime-1} \circ x) u_{\mathbf{R}}(\mathbf{R}^{\prime\prime}) d\mathbf{R}^{\prime\prime}$$
(49)

$$= \operatorname{Aug}[p_x](x). \tag{50}$$

A.3 ROTATIONAL AUGMENTATION DOES NOT AFFECT EQUIVARIANT DENOISERS

Using the equivariance of D and the fact that for any rotation R, we have $\mathbf{R}^T \mathbf{R} = \mathbb{I}_{3\times 3}$:

$$||D(\mathbf{R}(x+\eta)) - \mathbf{R}x||^2 = ||\mathbf{R}D(x+\eta) - \mathbf{R}x||^2$$
(51)

$$= \left\| \mathbf{R}(D(x+\eta) - x) \right\|^2 \tag{52}$$

$$= (\mathbf{R}(D(x+\eta) - x))^T \mathbf{R}(D(x+\eta) - x)$$
(53)

$$= (D(x+\eta) - x))^T \mathbf{R}^T \mathbf{R} (D(x+\eta) - x)$$
(54)

$$= (D(x+\eta) - x))^{T} (D(x+\eta) - x)$$
 (55)

$$= \|(D(x+\eta) - x)\|^2 \tag{56}$$

Hence, the loss $l_{\text{no-aug}}(D)$ is invariant under rotations **R**. Thus, if D is equivariant:

$$l_{\text{no-aug}}(D) = \mathbb{E}_{\mathbf{R} \sim u_{\mathbf{R}}} \mathbb{E}_{x \sim p_x} \mathbb{E}_{\eta \sim p_\eta} \left\| D(\mathbf{R}(x+\eta)) - \mathbf{R}x \right\|^2 = l_{\text{aug}}(D)$$
 (57)

B NO PERFECT DENOISER EXISTS WITH ROTATIONAL AUGMENTATION

Suppose we only had one sample x_0 where $||x_0|| > 0$. Hence, our distribution is a delta function $p_x(x) = \delta(x - x_0)$. Fix a noise level $\sigma > 0$. Here, we argue why a perfect denoiser cannot exist².

In this setting, assume that there exists a perfect denoiser D_{perf} :

$$D_{\text{perf}}(\mathbf{R} \circ (x_0 + \sigma \eta)) = \mathbf{R} \circ x_0 \tag{58}$$

for all rotations **R** and noise η . Such a D_{perf} obtains zero loss: $l_{aug}(D_{perf}) = 0$.

We show that such a D_{perf} cannot exist, by contradiction. Set $\mathbf{R} = \mathbb{I}$ in Equation 58, to see that $D_{\text{perf}}(x_0 + \sigma \eta) = x_0$ for all instantiations of η . Fix some noise η_0 arbitrarily. Now, consider any non-identity rotation \mathbf{R} . Let $\eta_{\mathbf{R}}$ be such that:

$$\mathbf{R} \circ (x_0 + \sigma \eta_{\mathbf{R}}) = x_0 + \sigma \eta_0 \quad \Longrightarrow \quad \eta_{\mathbf{R}} = \frac{\mathbf{R}^{\top} \circ (x_0 + \sigma \eta_0) - x_0}{\sigma}$$
 (59)

where we used the fact that **R** is orthonormal. Now, setting $\eta = \eta_{\mathbf{R}}$ in Equation 58:

$$D_{\text{perf}}(\mathbf{R} \circ (x_0 + \sigma \eta_{\mathbf{R}})) = \mathbf{R} \circ x_0. \tag{60}$$

But from the definition of $\eta_{\mathbf{R}}$, we have:

$$D_{\text{perf}}(\mathbf{R} \circ (x_0 + \sigma \eta_{\mathbf{R}})) = D_{\text{perf}}(x_0 + \sigma \eta_0) = x_0. \tag{61}$$

As \mathbf{R} is not the identity, we have a contradiction. Thus, D_{perf} cannot exist.

²This argument can be made rigorous to allow for exceptions of zero measure. We do this in Appendix B.1, but ignore such exceptions for clarity here.

B.1 NO PERFECT DENOISER EXISTS WITH ROTATIONAL AUGMENTATION

We can formalize the argument of Appendix B to include exceptions of measure 0.

Assume that there exists a perfect denoiser D_{perf} :

$$D_{\text{perf}}(\mathbf{R} \circ (x_0 + \sigma \eta)) = \mathbf{R} \circ x_0 \tag{62}$$

for all rotations \mathbf{R} and noise η , except on a set S of measure 0 over $SO(3) \times \mathbb{R}^{N \times 3}$. Now, define the family of sets:

$$R(y) = \{ (\mathbf{R}, \eta) : \mathbf{R} \circ (x_0 + \sigma \eta) = y \}$$
(63)

for each $y \in \mathbb{R}^{N \times 3}$. It is easy to verify that $\{R(y)\}_{y \in \mathbb{R}^{N \times 3}}$ is a partition of the space $SO(3) \times \mathbb{R}^{N \times 3}$. Further, each R(y) is diffeomorphic to SO(3), since we can always find a η for every \mathbf{R} to satisfy $\mathbf{R} \circ (x_0 + \sigma \eta) = y$. Thus, we have $\mu_{SO(3)}(R(y)) = 1$ where $\mu_{SO(3)}$ is the Haar measure over SO(3).

Thus, we can measure any measurable set A by integrating the measure of its intersections with each R(y). Formally, by the co-area formula, where μ represents the product measure over $SO(3) \times \mathbb{R}^{N \times 3}$:

$$\mu(A) = \int_{y \in \mathbb{R}^{N \times 3}} \mu_{SO(3)}(A \cap R(y))J(y)dy \tag{64}$$

where J(y) > 0 is the Jacobian factor. (Essentially, this is the 'change of variables' formula.) Now, applying this to S with $\mu(S) = 0$, we see that:

$$\int_{y \in \mathbb{R}^{N \times 3}} \mu_{SO(3)}(S \cap R(y)) J(y) dy = 0$$
(65)

$$\implies \mu_{SO(3)}(S \cap R(y)) = 0 \text{ for almost every } y \in \mathbb{R}^{N \times 3}$$
 (66)

Pick any such y. Then,

$$\mu_{SO(3)}(R(y) - S) = \mu_{SO(3)}(R(y)) - \mu_{SO(3)}(S \cap R(y)) = 1 - 0 = 1.$$
(67)

Thus, for this particular y, $\mu_{SO(3)}(R(y)-S)=1>0 \implies R(y)-S$ is uncountable, and has infinitely many points. In particular, there exist atleast two different points (\mathbf{R}_1,η_1) and (\mathbf{R}_2,η_2) in R(y)-S such that $\mathbf{R}_1\neq\mathbf{R}_2$. Now, for each of these two points:

$$\mathbf{R}_1 \circ (x_0 + \sigma \eta_1) = y = \mathbf{R}_2 \circ (x_0 + \sigma \eta_2). \tag{68}$$

But, since (\mathbf{R}_1, η_1) and (\mathbf{R}_2, η_2) in R(y) - S (and hence, not in S), we must have perfect denoising for the corresponding inputs:

$$\mathbf{R}_{1} \circ x_{0} = D_{\text{perf}}(\mathbf{R}_{1} \circ (x_{0} + \sigma \eta_{1})) = D_{\text{perf}}(y) = D_{\text{perf}}(\mathbf{R}_{2} \circ (x_{0} + \sigma \eta_{2})) = \mathbf{R}_{2} \circ x_{0}$$
 (69)

which is a contradiction as $||x_0|| > 0$ and $\mathbf{R}_1 \neq \mathbf{R}_2$. Thus, perfect denoising is impossible.

B.2 THE OPTIMAL DENOISER IN THE SINGLE SAMPLE SETTING

In the single sample case where $p_x(x) = \delta(x - x_0)$, using the isotropy of the Gaussian p_n :

$$l_{\text{aug}}(D) = \mathbb{E}_{\mathbf{R} \sim u_{\mathbf{R}}} \mathbb{E}_{\eta \sim \mathcal{N}(0, \sigma^2 \mathbb{I}_{N \times 3})} \left\| D(\mathbf{R}(x_0 + \eta)) - \mathbf{R}x_0 \right\|^2$$
(70)

$$= \mathbb{E}_{\mathbf{R} \sim u_{\mathbf{R}}} \mathbb{E}_{\eta \sim \mathcal{N}(0, \sigma^2 \mathbb{I}_{N \times 3})} \|D(\mathbf{R}x_0 + \eta) - \mathbf{R}x_0\|^2$$
(71)

$$= \mathbb{E}_{\mathbf{R} \sim u_{\mathbf{R}}} \mathbb{E}_{y \sim \mathcal{N}(\mathbf{R}x_0, \sigma^2 \mathbb{I}_{N \times 3})} \|D(y) - \mathbf{R}x_0\|^2$$
(72)

$$= \int_{SO(3)} \left(\int_{\mathbb{R}^{N\times3}} \|D(y) - \mathbf{R}x_0\|^2 \mathcal{N}(y; \mathbf{R}x_0, \sigma^2 \mathbb{I}_{N\times3}) dy \right) u_{\mathbf{R}}(\mathbf{R}) d\mathbf{R}$$
 (73)

$$= \int_{\mathbb{R}^{N\times3}} \left(\int_{SO(3)} \|D(y) - \mathbf{R}x_0\|^2 \mathcal{N}(y; \mathbf{R}x_0, \sigma^2 \mathbb{I}_{N\times3}) u_{\mathbf{R}}(\mathbf{R}) d\mathbf{R} \right) dy$$
 (74)

$$= \int_{\mathbb{R}^{N\times 3}} l_{\text{aug}}(D; y, \sigma) dy \tag{75}$$

where we define:

$$l_{\text{aug}}(D; y, \sigma) = \int_{SO(3)} \|D(y) - \mathbf{R}x_0\|^2 \mathcal{N}(y; \mathbf{R}x_0, \sigma^2 \mathbb{I}_{N \times 3}) u_{\mathbf{R}}(\mathbf{R}) d\mathbf{R}$$
 (76)

$$= \mathbb{E}_{\mathbf{R} \sim u_{\mathbf{R}}} \|D(y) - \mathbf{R}x_0\|^2 \mathcal{N}(y; \mathbf{R}x_0, \sigma^2 \mathbb{I}_{N \times 3})$$
(77)

Note that $l_{\text{aug}}(D;y)$ is non-negative for all y. Thus, the optimal denoiser D^* should minimize $l_{\text{aug}}(D;y)$ for each possible y. Taking the gradient of $l_{\text{aug}}(D;y)$ with respect to D(y) and setting it to 0:

$$\nabla_{D(y)}l_{\text{aug}}(D;y,\sigma) = 0 \tag{78}$$

$$\implies \mathbb{E}_{\mathbf{R} \sim u_{\mathbf{R}}} \left[2(D^*(y) - \mathbf{R}x_0) \mathcal{N}(y; \mathbf{R}x_0, \sigma^2 \mathbb{I}_{N \times 3}) \right] = 0$$
 (79)

$$\implies D^*(y) = \frac{\mathbb{E}_{\mathbf{R} \sim u_{\mathbf{R}}}[\mathbf{R}x_0 \, \mathcal{N}(y; \mathbf{R}x_0, \sigma^2 \mathbb{I}_{N \times 3})]}{\mathbb{E}_{\mathbf{R} \sim u_{\mathbf{R}}}[\mathcal{N}(y; \mathbf{R}x_0, \sigma^2 \mathbb{I}_{N \times 3})]}$$
(80)

This is the optimal denoiser in the single sample setting! We can rewrite this a bit:

$$D^{*}(y) = \frac{\int_{SO(3)} \mathbf{R} x_{0} \mathcal{N}(y; \mathbf{R} x_{0}, \sigma^{2} \mathbb{I}_{N \times 3}) u_{\mathbf{R}}(\mathbf{R}) d\mathbf{R}}{\int_{SO(3)} \mathcal{N}(y; \mathbf{R} x_{0}, \sigma^{2} \mathbb{I}_{N \times 3}) u_{\mathbf{R}}(\mathbf{R}) d\mathbf{R}}$$
(81)

$$= \frac{\int_{SO(3)} \mathbf{R} x_0 \mathcal{N}(y; \mathbf{R} x_0, \sigma^2 \mathbb{I}_{N \times 3}) u_{\mathbf{R}}(\mathbf{R}) d\mathbf{R}}{\int_{SO(3)} \mathcal{N}(y; \mathbf{R}' x_0, \sigma^2 \mathbb{I}_{N \times 3}) u_{\mathbf{R}}(\mathbf{R}') d\mathbf{R}'}$$
(82)

$$= \int_{SO(3)} \mathbf{R} x_0 \frac{\mathcal{N}(y; \mathbf{R} x_0, \sigma^2 \mathbb{I}_{N \times 3}) u_{\mathbf{R}}(\mathbf{R}) d\mathbf{R}}{\int_{SO(3)} \mathcal{N}(y; \mathbf{R}' x_0, \sigma^2 \mathbb{I}_{N \times 3}) u_{\mathbf{R}}(\mathbf{R}') d\mathbf{R}'}$$
(83)

$$= \int_{SO(3)} \mathbf{R} x_0 \ p(\mathbf{R} \mid y, x_0) d\mathbf{R}$$
 (84)

$$= \mathbb{E}_{\mathbf{R} \sim p(\mathbf{R} \mid y, x_0)}[\mathbf{R}x_0] \tag{85}$$

as:

$$p(\mathbf{R} \mid y, x_0) = \frac{\mathcal{N}(y; \mathbf{R}x_0, \sigma^2 \mathbb{I}_{N \times 3}) u_{\mathbf{R}}(\mathbf{R})}{\int_{SO(3)} \mathcal{N}(y; \mathbf{R}'x_0, \sigma^2 \mathbb{I}_{N \times 3}) u_{\mathbf{R}}(\mathbf{R}') d\mathbf{R}'}$$
(86)

is the distribution over rotations $\mathbf R$ conditional on y, because:

$$p(y \mid \mathbf{R}, x_0) = \mathcal{N}(y; \mathbf{R}x_0, \sigma^2 \mathbb{I}_{N \times 3})$$
(87)

and Bayes' rule:

$$p(\mathbf{R} \mid y, x_0) = \frac{p(y, \mathbf{R} \mid x_0)}{p(y \mid x_0)} = \frac{p(y \mid \mathbf{R}, x_0)p(\mathbf{R} \mid x_0)}{\int_{SO(3)} p(y \mid \mathbf{R}', x_0)p(\mathbf{R}' \mid x_0)d\mathbf{R}'}$$
(88)

and noticing that $p(\mathbf{R} \mid x_0) = u_{\mathbf{R}}(\mathbf{R})$.

B.3 THE OPTIMAL DENOISER IN THE GENERAL SETTING

The same idea and calculations from Section 3.1 hold in the general setting, where p_x is arbitrary.

Using the isotropy of the Gaussian p_n :

$$l_{\text{aug}}(D) = \mathbb{E}_{\mathbf{R} \sim u_{\mathbf{R}}} \mathbb{E}_{x \sim p_x} \mathbb{E}_{\eta \sim \mathcal{N}(0, \sigma^2 \mathbb{I}_{N \times 3})} \|D(\mathbf{R}(x+\eta)) - \mathbf{R} \circ x\|^2$$
(89)

$$= \mathbb{E}_{\mathbf{R} \sim u_{\mathbf{R}}} \mathbb{E}_{x \sim p_x} \mathbb{E}_{\eta \sim \mathcal{N}(0, \sigma^2 \mathbb{I}_{N \times 3})} \| D(\mathbf{R} \circ x + \eta) - \mathbf{R} \circ x \|^2$$
(90)

$$= \mathbb{E}_{\mathbf{R} \sim u_{\mathbf{R}}} \mathbb{E}_{x \sim p_{x}} \mathbb{E}_{y \sim \mathcal{N}(\mathbf{R} \circ x, \sigma^{2} \mathbb{I}_{N \times 3})} \|D(y) - \mathbf{R} \circ x\|^{2}$$
(91)

$$= \int_{SO(3)} \int_{\mathbb{R}^{N\times 3}} \left(\int_{\mathbb{R}^{N\times 3}} \|D(y) - \mathbf{R} \circ x_0\|^2 \mathcal{N}(y; \mathbf{R} \circ x, \sigma^2 \mathbb{I}_{N\times 3}) dy \right) p_x(x) dx \ u_{\mathbf{R}}(\mathbf{R}) d\mathbf{R}$$
(92)

$$= \int_{\mathbb{R}^{N\times3}} \left(\int_{\mathbb{R}^{N\times3}} \left(\int_{SO(3)} \|D(y) - \mathbf{R} \circ x\|^2 \mathcal{N}(y; \mathbf{R} \circ x, \sigma^2 \mathbb{I}_{N\times3}) u_{\mathbf{R}}(\mathbf{R}) d\mathbf{R} \right) p_x(x) dx \right) dy$$
(93)

$$= \int_{\mathbb{R}^{N\times 3}} l_{\text{aug}}(D; y, \sigma) dy \tag{94}$$

where:

$$l_{\text{aug}}(D; y, \sigma) = \int_{\mathbb{R}^{N \times 3}} \int_{SO(3)} \|D(y) - \mathbf{R} \circ x\|^2 \mathcal{N}(y; \mathbf{R} \circ x, \sigma^2 \mathbb{I}_{N \times 3}) u_{\mathbf{R}}(\mathbf{R}) d\mathbf{R} p_x(x) dx$$
(95)
$$= \mathbb{E}_{x \sim p_x} \mathbb{E}_{\mathbf{R} \sim u_{\mathbf{R}}} \|D(y) - \mathbf{R} \circ x\|^2 \mathcal{N}(y; \mathbf{R} \circ x, \sigma^2 \mathbb{I}_{N \times 3})$$
(96)

Note that $l_{\text{aug}}(D;y)$ is non-negative for all y. Thus, the optimal denoiser D^* should minimize

 $l_{\text{aug}}(D;y)$ for each possible y. Taking the gradient of $l_{\text{aug}}(D;y)$ with respect to D(y) and setting it to 0:

$$\nabla_{D(y)} l_{\text{aug}}(D; y, \sigma) = 0 \tag{97}$$

$$\implies \mathbb{E}_{x \sim p_x} \mathbb{E}_{\mathbf{R} \sim u_{\mathbf{R}}} \left[2(D^*(y) - \mathbf{R} \circ x) \mathcal{N}(y; \mathbf{R} \circ x, \sigma^2 \mathbb{I}_{N \times 3}) \right] = 0$$
 (98)

$$\implies D^*(y) = \frac{\mathbb{E}_{x \sim p_x} \mathbb{E}_{\mathbf{R} \sim u_{\mathbf{R}}} [\mathbf{R} \circ x \, \mathcal{N}(y; \mathbf{R} \circ x, \sigma^2 \mathbb{I}_{N \times 3})]}{\mathbb{E}_{x \sim p_x} \mathbb{E}_{\mathbf{R} \sim u_{\mathbf{R}}} [\mathcal{N}(y; \mathbf{R} \circ x, \sigma^2 \mathbb{I}_{N \times 3})]}$$
(99)

which clearly specializes to Equation 81 in the single sample setting. As before, we can write this as:

$$D^{*}(y) = \frac{\mathbb{E}_{x \sim p_{x}} \mathbb{E}_{\mathbf{R} \sim u_{\mathbf{R}}} \mathbf{R} \circ x \, \mathcal{N}(y; \mathbf{R} \circ x, \sigma^{2} \mathbb{I}_{N \times 3})}{\mathbb{E}_{x \sim p_{x}} \mathbb{E}_{\mathbf{R} \sim u_{\mathbf{R}}} \mathcal{N}(y; \mathbf{R} \circ x, \sigma^{2} \mathbb{I}_{N \times 3})}$$
(100)

$$= \frac{\int_{SO(3)} \int_{\mathbb{R}^{N\times3}} \mathbf{R} \circ x \, \mathcal{N}(y; \mathbf{R} \circ x, \sigma^2 \mathbb{I}_{N\times3}) p_x(x) u_{\mathbf{R}}(\mathbf{R}) dx d\mathbf{R}}{\int_{SO(3)} \int_{\mathbb{R}^{N\times3}} \mathcal{N}(y; \mathbf{R}'x', \sigma^2 \mathbb{I}_{N\times3}) p_x(x') u_{\mathbf{R}}(\mathbf{R}') dx' d\mathbf{R}'}$$
(101)

$$= \int_{SO(3)} \int_{\mathbb{R}^{N\times 3}} \mathbf{R} \circ x \frac{\mathcal{N}(y; \mathbf{R} \circ x, \sigma^2 \mathbb{I}_{N\times 3}) p_x(x) u_{\mathbf{R}}(\mathbf{R}) dx d\mathbf{R}}{\int_{SO(3)} \int_{\mathbb{R}^{N\times 3}} \mathcal{N}(y; \mathbf{R}'x', \sigma^2 \mathbb{I}_{N\times 3}) p_x(x') u_{\mathbf{R}}(\mathbf{R}') dx' d\mathbf{R}'}$$
(102)

$$= \int_{SO(3)} \int_{\mathbb{R}^{N\times 3}} \mathbf{R} \circ x \, p(x, \mathbf{R} \mid y, \sigma) dx d\mathbf{R}$$
 (103)

$$= \mathbb{E}_{x,\mathbf{R} \sim p(x,\mathbf{R} \mid y,\sigma)}[\mathbf{R} \circ x] \tag{104}$$

$$= \mathbb{E}_{x \sim p(x \mid y, \sigma)} [\mathbb{E}_{\mathbf{R} \sim p(\mathbf{R} \mid y, x, \sigma)} [\mathbf{R} \circ x]]$$
 (105)

$$= \mathbb{E}_{x \sim p(x \mid y, \sigma)}[D^*(y; x)] \tag{106}$$

as the conditional probability distribution $p(x, \mathbf{R} \mid y, \sigma)$ over both point clouds x and rotations \mathbf{R} is:

$$p(x, \mathbf{R} \mid y, \sigma) = \frac{p(y \mid \mathbf{R}, x, \sigma)p(x)p(\mathbf{R})}{\int_{x} \int_{\mathbf{R}} p(y \mid \mathbf{R}, x, \sigma)p(x)p(\mathbf{R})}$$
(107)

$$= \frac{\mathcal{N}(y; \mathbf{R} \circ x, \sigma^2 \mathbb{I}_{N \times 3}) p_x(x) u_{\mathbf{R}}(\mathbf{R})}{\int_{SO(3)} \int_{\mathbb{R}^{N \times 3}} \mathcal{N}(y; \mathbf{R}' x', \sigma^2 \mathbb{I}_{N \times 3}) p_x(x') u_{\mathbf{R}}(\mathbf{R}') dx' d\mathbf{R}'}$$
(108)

Note that the marginal distribution over \mathbf{R} under $p(x, \mathbf{R} \mid y, \sigma)$ is indeed $p(\mathbf{R} \mid y, x, \sigma)$ as derived in Equation 10. Note that:

$$p(\mathbf{R} \mid y, x, \sigma) = \frac{\mathcal{N}(y; \mathbf{R} \circ x, \sigma^2 \mathbb{I}_{N \times 3}) u_{\mathbf{R}}(\mathbf{R})}{\int_{SO(3)} \mathcal{N}(y; \mathbf{R}' x, \sigma^2 \mathbb{I}_{N \times 3}) u_{\mathbf{R}}(\mathbf{R}') d\mathbf{R}'}$$
(109)

because:

$$p(y \mid \mathbf{R}, x, \sigma) = \mathcal{N}(y; \mathbf{R} \circ x, \sigma^2 \mathbb{I}_{N \times 3})$$
(110)

and Bayes' rule:

$$p(\mathbf{R} \mid y, x) = \frac{p(y, \mathbf{R} \mid x)}{p(y \mid x)} = \frac{p(y \mid \mathbf{R}, x, \sigma)p(\mathbf{R} \mid x)}{\int_{SO(3)} p(y \mid \mathbf{R}', x)p(\mathbf{R}' \mid x)d\mathbf{R}'}$$
(111)

and noticing that $p(\mathbf{R} \mid x) = u_{\mathbf{R}}(\mathbf{R})$.

B.4 CONNECTION TO THE MATRIX FISHER DISTRIBUTION

Here, we show that $p(\mathbf{R} \mid y; x_0, \sigma)$ belongs to the family of Matrix Fisher distributions:

$$p(\mathbf{R} \mid y; x_0, \sigma) \propto \mathcal{N}(y; \mathbf{R} \circ x_0, \sigma^2 \mathbb{I}_{N \times 3}) u_{\mathbf{R}}(\mathbf{R})$$
 (112)

$$\propto \exp\left(-\frac{\|y - \mathbf{R} \circ x_0\|^2}{2\sigma^2}\right) \tag{113}$$

$$\propto \exp\left(-\frac{\|y\|^2 + \|\mathbf{R} \circ x_0\|^2 - 2\operatorname{Tr}[y^T(\mathbf{R} \circ x_0)]}{2\sigma^2}\right)$$
(114)

$$\propto \exp\left(-\frac{\|y\|^2 + \|x_0\|^2 - 2\operatorname{Tr}[y^T(\mathbf{R} \circ x_0)]}{2\sigma^2}\right)$$
 (115)

$$\propto \exp\left(\frac{\text{Tr}[y^T(\mathbf{R} \circ x_0)]}{\sigma^2}\right)$$
 (116)

$$\propto \exp\left(\frac{\text{Tr}[y^T(x_0\mathbf{R}^T)]}{\sigma^2}\right)$$
 (117)

$$\propto \exp\left(\frac{\text{Tr}[\mathbf{R}^T y^T x_0]}{\sigma^2}\right) \tag{118}$$

$$\propto \exp\left(\frac{\text{Tr}[(y^T x_0)^T \mathbf{R}]}{\sigma^2}\right)$$
 (119)

$$\propto \exp\left(\operatorname{Tr}\left[\left(\frac{y^T x_0}{\sigma^2}\right)^T \mathbf{R}\right]\right)$$
 (120)

Hence, $p(\mathbf{R} \mid y; x_0, \sigma) = \mathrm{MF}(\mathbf{R}; \frac{y^T x_0}{\sigma^2}).$

B.5 THE OPTIMAL CONDITIONAL DENOISER IS SO(3)-Equivariant

Here, we show the that the optimal denoiser D^* is indeed *equivariant* under rotations of y. For an arbitrary rotation \mathbf{R}' :

$$D^{*}(\mathbf{R}'y; x_{0}, \sigma) = \frac{\mathbb{E}_{\mathbf{R} \sim u_{\mathbf{R}}}[\mathbf{R} \circ x_{0} \mathcal{N}(\mathbf{R}'y; \mathbf{R} \circ x_{0}, \sigma^{2} \mathbb{I}_{N \times 3})]}{\mathbb{E}_{\mathbf{R} \sim u_{\mathbf{R}}}[\mathcal{N}(\mathbf{R}'y; \mathbf{R} \circ x_{0}, \sigma^{2} \mathbb{I}_{N \times 3})]}$$
(121)

$$= \frac{\mathbb{E}_{\mathbf{R} \sim u_{\mathbf{R}}}[\mathbf{R} \circ x_0 \,\mathcal{N}(y; (\mathbf{R}')^{-1}\mathbf{R} \circ x_0, \sigma^2 \mathbb{I}_{N \times 3})]}{\mathbb{E}_{\mathbf{R} \sim u_{\mathbf{R}}}[\mathcal{N}(y; (\mathbf{R}')^{-1}\mathbf{R} \circ x_0, \sigma^2 \mathbb{I}_{N \times 3})]}$$
(122)

$$= \frac{\mathbb{E}_{\mathbf{R} \sim u_{\mathbf{R}}}[\mathbf{R}'((\mathbf{R}')^{-1}\mathbf{R})x_0 \,\mathcal{N}(y; ((\mathbf{R}')^{-1}\mathbf{R})x_0, \sigma^2 \mathbb{I}_{N \times 3})]}{\mathbb{E}_{\mathbf{R} \sim u_{\mathbf{R}}}[\mathcal{N}(y; ((\mathbf{R}')^{-1}\mathbf{R})x_0, \sigma^2 \mathbb{I}_{N \times 3})]}$$
(123)

$$= \frac{\mathbb{E}_{\mathbf{R}'' \sim u_{\mathbf{R}}}[\mathbf{R}'\mathbf{R}''x_{0} \mathcal{N}(y; \mathbf{R}''x_{0}, \sigma^{2}\mathbb{I}_{N \times 3})]}{\mathbb{E}_{\mathbf{R}'' \sim u_{\mathbf{R}}}[\mathcal{N}(y; \mathbf{R}''x_{0}, \sigma^{2}\mathbb{I}_{N \times 3})]}$$
(124)

$$= \mathbf{R}' \frac{\mathbb{E}_{\mathbf{R}'' \sim u_{\mathbf{R}}} [\mathbf{R}'' x_0 \, \mathcal{N}(y; \mathbf{R}'' x_0, \sigma^2 \mathbb{I}_{N \times 3})]}{\mathbb{E}_{\mathbf{R}'' \sim u_{\mathbf{R}}} [\mathcal{N}(y; \mathbf{R}'' x_0, \sigma^2 \mathbb{I}_{N \times 3})]}$$
(125)

$$= \mathbf{R}' D^*(y; x_0, \sigma) \tag{126}$$

where we used the fact that $u_{\mathbf{R}}$ is uniform so $\mathbf{R}'' \equiv (\mathbf{R}')^{-1}\mathbf{R}$ is also distributed as $u_{\mathbf{R}}$, by the invariance of the Haar measure.

Next, we show that the optimal conditional denoiser D^* is indeed *invariant* under rotations of conditioning x_0 . For an arbitrary rotation \mathbf{R}' :

$$D^{*}(y; \mathbf{R}'x_{0}, \sigma) = \frac{\mathbb{E}_{\mathbf{R} \sim u_{\mathbf{R}}}[\mathbf{R} \circ \mathbf{R}'x_{0} \,\mathcal{N}(y; \mathbf{R} \circ \mathbf{R}'x_{0}, \sigma^{2}\mathbb{I}_{N \times 3})]}{\mathbb{E}_{\mathbf{R} \sim u_{\mathbf{R}}}[\mathcal{N}(y; \mathbf{R} \circ \mathbf{R}'x_{0}, \sigma^{2}\mathbb{I}_{N \times 3})]}$$
(127)

$$= \frac{\mathbb{E}_{\mathbf{R} \sim u_{\mathbf{R}}}[(\mathbf{R}\mathbf{R}')x_{0} \mathcal{N}(y; (\mathbf{R}\mathbf{R}') \circ x_{0}, \sigma^{2}\mathbb{I}_{N \times 3})]}{\mathbb{E}_{\mathbf{R} \sim u_{\mathbf{R}}}[\mathcal{N}(y; (\mathbf{R}\mathbf{R}') \circ x_{0}, \sigma^{2}\mathbb{I}_{N \times 3})]}$$
(128)

$$= \frac{\mathbb{E}_{\mathbf{R''} \sim u_{\mathbf{R}}}[\mathbf{R''} x_0 \, \mathcal{N}(y; \mathbf{R''} \circ x_0, \sigma^2 \mathbb{I}_{N \times 3})]}{\mathbb{E}_{\mathbf{R} \sim u_{\mathbf{R}}}[\mathcal{N}(y; \mathbf{R''} \circ x_0, \sigma^2 \mathbb{I}_{N \times 3})]}$$
(129)

$$= D^*(y; x_0, \sigma) \tag{130}$$

where we again used the fact that $u_{\mathbf{R}}$ is uniform so $\mathbf{R}'' \equiv \mathbf{R}\mathbf{R}'$ is also distributed as $u_{\mathbf{R}}$, by the invariance of the Haar measure.

B.6 ROTATIONAL ALIGNMENT COMMUTES WITH ROTATIONAL AUGMENTATION

Here, we show that alignment commutes with the rotation \mathbf{R}_{aug} used for augmentation. In particular, the alignment procedure returns $\mathbf{R}^*(\mathbf{R}_{\text{aug}} \circ y, \mathbf{R}_{\text{aug}} \circ x) = \mathbf{R}_{\text{aug}} \mathbf{R}^*(y, x) \mathbf{R}_{\text{aug}}^T$. This is because:

$$\mathbf{R}^{*}(\mathbf{R}_{\text{aug}} \circ y, \mathbf{R}_{\text{aug}} \circ x) = \underset{\mathbf{R} \in SO(3)}{\operatorname{argmin}} \| \mathbf{R}_{\text{aug}} \circ y - \mathbf{R} \mathbf{R}_{\text{aug}} \circ x \|$$
(131)

$$= \underset{\mathbf{R} \in SO(3)}{\operatorname{argmin}} \| y - \mathbf{R}_{\operatorname{aug}}^T \mathbf{R} \mathbf{R}_{\operatorname{aug}} \circ x \|$$
 (132)

$$\implies \mathbf{R}_{\text{aug}}^T \mathbf{R}^* (\mathbf{R}_{\text{aug}} \circ y, \mathbf{R}_{\text{aug}} \circ x) \mathbf{R}_{\text{aug}} = \mathbf{R}^* (y, x)$$
(133)

$$\implies \mathbf{R}^*(\mathbf{R}_{\text{aug}} \circ y, \mathbf{R}_{\text{aug}} \circ x) = \mathbf{R}_{\text{aug}} \mathbf{R}^*(y, x) \mathbf{R}_{\text{aug}}^T$$
(134)

Thus, on aligning $\mathbf{R}_{\mathrm{aug}} \circ x$ to $\mathbf{R}_{\mathrm{aug}} \circ y$, we get $\mathbf{R}^*(\mathbf{R}_{\mathrm{aug}}y, \mathbf{R}_{\mathrm{aug}}x) \circ (\mathbf{R}_{\mathrm{aug}}x) = \mathbf{R}_{\mathrm{aug}}\mathbf{R}^*(y, x)\mathbf{R}_{\mathrm{aug}}^T\mathbf{R}_{\mathrm{aug}} \circ x = \mathbf{R}_{\mathrm{aug}}\mathbf{R}^*(y, x) \circ x$.

B.7 AVERAGING AN ESTIMATOR INDUCES AN EQUIVALENT MATCHING LOSS

Here, we show that averaging an estimator D_{est} gives us an equivalent matching loss from the perspective of minimization with respect to D. Formally, for any estimator D_{est} we have:

$$l_{\text{est}}(D; \mathbb{E}_{\mathbf{R} \sim p(\mathbf{R} \mid y, x, \sigma)}[D_{\text{est}}]) = l_{\text{est}}(D; D_{\text{est}}) + C$$
(135)

where C is a constant that does not depend on D. We have:

$$l_{\rm est}(D;D_{\rm est})$$

$$= \mathbb{E}_{\sigma \sim p_{\sigma}} \mathbb{E}_{y \sim p(y|\sigma)} \mathbb{E}_{x \sim p(x \mid y, \sigma)} \mathbb{E}_{\mathbf{R} \sim p(\mathbf{R} \mid y, x, \sigma)} [\|D(y; \sigma) - D_{\text{est}}(y; x, \mathbf{R}, \sigma)\|^{2}]$$
(136)

$$= \mathbb{E}_{\sigma} \mathbb{E}_{y} \mathbb{E}_{x} \mathbb{E}_{\mathbf{R}} [\|D(y; \sigma) - D_{\text{est}}(y; x, \mathbf{R}, \sigma)\|^{2}]$$
(137)

$$= \mathbb{E}_{\sigma} \mathbb{E}_{y} \mathbb{E}_{x} \mathbb{E}_{\mathbf{R}}[\|D(y;\sigma) - \mathbb{E}_{\mathbf{R}}[D_{\text{est}}(y;x,\mathbf{R},\sigma)] + \mathbb{E}_{\mathbf{R}}[D_{\text{est}}(y;x,\mathbf{R},\sigma)] - D_{\text{est}}(y;x,\mathbf{R},\sigma)\|^{2}]$$
(138)

$$= \mathbb{E}_{\sigma} \mathbb{E}_{y} \mathbb{E}_{\mathbf{R}} \mathbb{E}_{\mathbf{R}} [\|D(y;\sigma) - \mathbb{E}_{\mathbf{R}} [D_{\text{est}}(y;x,\mathbf{R},\sigma)]\|^{2} + \|\mathbb{E}_{\mathbf{R}} [D_{\text{est}}(y;x,\mathbf{R},\sigma)] - D_{\text{est}}(y;x,\mathbf{R},\sigma)]^{2}$$

$$+ 2(D(y;\sigma) - \mathbb{E}_{\mathbf{R}} [D_{\text{est}}(y;x,\mathbf{R},\sigma)])^{\top} (\mathbb{E}_{\mathbf{R}} [D_{\text{est}}(y;x,\mathbf{R},\sigma)] - D_{\text{est}}(y;x,\mathbf{R},\sigma)]$$
(139)

where we omit the explicit distributions for clarity. Now, focusing on the last term:

$$\mathbb{E}_{\mathbf{R}}[2(D(y;\sigma) - \mathbb{E}_{\mathbf{R}}[D_{\text{est}}(y;x,\mathbf{R},\sigma)])^{\top}(\mathbb{E}_{\mathbf{R}}[D_{\text{est}}(y;x,\mathbf{R},\sigma)] - D_{\text{est}}(y;x,\mathbf{R},\sigma))]$$
(140)

$$= 2(D(y;\sigma) - \mathbb{E}_{\mathbf{R}}[D_{\text{est}}(y;x,\mathbf{R},\sigma)])^{\top} \mathbb{E}_{\mathbf{R}}[(\mathbb{E}_{\mathbf{R}}[D_{\text{est}}(y;x,\mathbf{R},\sigma)] - D_{\text{est}}(y;x,\mathbf{R},\sigma))]$$
(141)

$$= 2(D(y;\sigma) - \mathbb{E}_{\mathbf{R}}[D_{\text{est}}(y;x,\mathbf{R},\sigma)])^{\top} (\mathbb{E}_{\mathbf{R}}[D_{\text{est}}(y;x,\mathbf{R},\sigma)] - \mathbb{E}_{\mathbf{R}}[D_{\text{est}}(y;x,\mathbf{R},\sigma)])$$
(142)

$$= 2(D(y;\sigma) - \mathbb{E}_{\mathbf{R}}[D_{\text{est}}(y;x,\mathbf{R},\sigma)])^{\mathsf{T}}\mathbf{0}$$
(143)

$$= 0. (144)$$

as the first term in the product is a constant with respect to **R**. Thus,

$$l_{\rm est}(D; D_{\rm est}) \tag{145}$$

$$= \mathbb{E}_{\sigma} \mathbb{E}_{y} \mathbb{E}_{x} \mathbb{E}_{\mathbf{R}} [\|D(y;\sigma) - \mathbb{E}_{\mathbf{R}} [D_{\text{est}}(y;x,\mathbf{R},\sigma)]\|^{2} + \|\mathbb{E}_{\mathbf{R}} [D_{\text{est}}(y;x,\mathbf{R},\sigma)] - D_{\text{est}}(y;x,\mathbf{R},\sigma)\|^{2}]$$
(146)

$$= l_{\text{est}}(D; \mathbb{E}_{\mathbf{R}}[D_{\text{est}}]) + \underbrace{\mathbb{E}_{\sigma} \mathbb{E}_{y} \mathbb{E}_{x} \mathbb{E}_{\mathbf{R}}[\|\mathbb{E}_{\mathbf{R}}[D_{\text{est}}(y; x, \mathbf{R}, \sigma)] - D_{\text{est}}(y; x, \mathbf{R}, \sigma)\|^{2}]}_{\text{independent of } D}.$$
(147)

as claimed.

C FOR A GENERAL MATRIX FISHER DISTRIBUTION

We note that the partition function $Z(F) = \int_{SO(3)} \exp(\text{Tr}[F^{\top}\mathbf{R}]) d\mathbf{R}$ gives all the information we need. In particular, taking derivatives of Z(F) allows us to calculate any necessary moments. For example,

$$\mathbb{E}_{\mathbf{R} \sim \mathrm{MF}(\mathbf{R}; F)}[\mathbf{R}] = \frac{\int_{SO(3)} \mathbf{R} \exp(\mathrm{Tr}[F^{\top}\mathbf{R}]) d\mathbf{R}}{Z(F)} = \frac{\frac{d}{dF} Z(F)}{Z(F)} = \frac{d}{dF} \ln Z(F)$$
(148)

using the trace derivative identity: $\frac{d}{dF} \operatorname{Tr}[F^{\top} \mathbf{R}] = \mathbf{R}$.

Now, we remove the explicit σ -dependence of $F = \frac{y^{\top}x}{\sigma^2}$, by defining $F' = y^{\top}x$ and $\lambda = \frac{1}{\sigma^2}$, so that $F = \lambda F'$. We are interested in computing $\mathbb{E}_{\mathbf{R} \sim \mathrm{MF}(\mathbf{R}; \lambda F')}[\mathbf{R}]$ in the limit of $\lambda \to \infty$.

Recall that we can always factorize $F' = USV^{\top}$ where $U, V \in SO(3)$ and $S = \text{diag}[s_1, s_2, s_3]$ where $s_1 \geq s_2 \geq |s_3|$, by the Singular Value Decomposition. In particular, we see that:

$$\operatorname{Tr}[F'^{\top}\mathbf{R}] = \operatorname{Tr}[VS^{\top}U^{\top}\mathbf{R}] = \operatorname{Tr}[S^{\top}U^{\top}\mathbf{R}V] = \operatorname{Tr}[S^{\top}(U^{\top}\mathbf{R}V)]$$
(149)

by the cyclic property of the trace. Since $U,V\in SO(3)$ it follows that Z(F')=Z(S) (by change of variables $\mathbf{R}\to U^{\top}\mathbf{R}V$) so we can restrict our calculations to the diagonal case .

Laplace's method provides a powerful tool to expand integrals of sharply peaked functions. The key idea is that only the neighborhood of a sharp peak has significant contributions and that such a region can be approximated with a Gaussian distribution. In our case, we seek to apply this method to $Z(\lambda S)$ in the limit of $\lambda \to \infty$.

As S is diagonal, it is easy to see that $\operatorname{argmax}_{\mathbf{R} \sim SO(3)}[\lambda \operatorname{Tr}[S\mathbf{R}]] = \mathbb{I}_{3\times 3}$. Hence, a natural parameterization to use is the exponential map expansion of SO(3) which expands around the identity. In this chart, we have parameters $\boldsymbol{\theta} = (\theta_x, \theta_y, \theta_z)$ and our rotation is given by

$$\mathbf{R}(\theta_x, \theta_y, \theta_z) = \exp(\theta_x R_x + \theta_y R_y + \theta_z R_z) \tag{150}$$

where R_x, R_y, R_z are the generators of x, y, z rotations. In this parameterization, the Haar measure can be found to be

$$\mu(\boldsymbol{\theta}) d\theta_x d\theta_y d\theta_z = \frac{1 - \cos(\|\boldsymbol{\theta}\|)}{4\pi^2 \|\boldsymbol{\theta}\|^2} d\theta_x d\theta_y d\theta_z.$$
 (151)

Next, we would like to expand the argument $\lambda A(\theta, S) = \lambda \operatorname{Tr}[S\mathbf{R}(\theta)]$ around $\theta = 0$. Because this is maximized at $\mathbf{R} = \mathbb{I}$ so $\theta = 0$, we obtain an expression of the form:

$$A(\boldsymbol{\theta}, S) = A_0(S) + \sum_{ij} A_{2,ij}(S)\theta_i\theta_j + \sum_{ijk} A_{3,ijk}(S)\theta_i\theta_j\theta_k + \dots$$
 (152)

where the indices i, j, k run over $\{x, y, z\}$.

Define $B(\theta, S, \lambda) \equiv \exp(\lambda(A(\theta, S) - A_0(S) - \sum_{ij} A_{2,ij}(S)\theta_i\theta_j))$. We can then write:

$$\exp(\lambda A(\boldsymbol{\theta}, S)) = \exp(\lambda A_0(S) + \sum_{ij} \lambda A_{2,ij}(S)\theta_i\theta_j) \exp(\lambda (A(\boldsymbol{\theta}, S) - A_0(S) - \sum_{ij} A_{2,ij}(S)\theta_i\theta_j))$$

$$= \exp(\lambda A_0(S) + \sum_{ij} \lambda A_{2,ij}(S)\theta_i\theta_j)B(\boldsymbol{\theta}, S, \lambda).$$

 To integrate over all of SO(3), we simply need to integrate over the domain $\{|\theta| < \pi\}$. Hence, we would like to evaluate:

$$\int_{|\boldsymbol{\theta}| < \pi} e^{\lambda A_0(S) + \sum_{ij} \lambda A_{2,ij}(S)\theta_i \theta_j} B(\boldsymbol{\theta}, S, \lambda) \mu(\boldsymbol{\theta}) d\boldsymbol{\theta}.$$
 (153)

Since $\theta=0$ is a local maxima, $A_{2,ij}(S)$ must be negative definite so the exponential component can be interpreted as a Gaussian. As $\lambda\to\infty$, this Gaussian becomes increasingly peaked; therefore, only the neighborhood around $\theta=0$ matters. Hence, we can expand $B(\theta,S,\lambda)\mu(\theta)$ around 0 to get:

$$B(\boldsymbol{\theta}, S, \lambda)\mu(\boldsymbol{\theta}) = M_0 + \sum_{ij} M_{2,ij}\theta_i\theta_j + \sum_{ijk} M_{3,ijk}(S, \lambda)\theta_i\theta_j\theta_k + \dots$$
 (154)

where the contributions up to second order can only come from the expansion of the measure (which has no S or λ dependence), and there is no first order term since the measure is symmetric around 0. Hence, Equation 153 becomes:

$$\int_{|\boldsymbol{\theta}| < \pi} e^{\lambda A_0(S) + \sum_{ij} \lambda A_{2,ij}(S)\theta_i \theta_j} \left(M_0 + \sum_{ij} M_{2,ij} \theta_i \theta_j + \sum_{ijk} M_{3,ijk}(S, \lambda) \theta_i \theta_j \theta_k + \ldots \right) d\boldsymbol{\theta}.$$
(155)

Finally, we note that as $\lambda \to \infty$, the Gaussian part has an increasingly sharp peak. Thus, for the expansion terms in Equation 155, the boundaries of integration matter increasingly less. Hence, replacing the domain $\{|\theta| < \pi\}$ with the larger domain $\{\theta \in \mathbb{R}^3\}$ gives us a good approximation for each of the expanded terms, but also gives us Gaussian integrals which are analytically evaluable.

Finally, we obtain an expression of the form:

$$Z(\lambda S) = N(S, \lambda) \left(1 + L_1(S) \frac{1}{\lambda} + L_2(S) \frac{1}{\lambda^2} + L_3(S) \frac{1}{\lambda^3} + \dots \right)$$
 (156)

where $N(S, \lambda)$ is a normalization term. The corresponding expected rotation can be computed as:

$$\mathbb{E}_{\mathbf{R} \sim \mathrm{MF}(\mathbf{R}; \lambda S)}[\mathbf{R}] = \frac{1}{\lambda} \operatorname{diag} \left[\frac{\partial \ln Z(\lambda S)}{\partial s_1}, \frac{\partial \ln Z(\lambda S)}{\partial s_1}, \frac{\partial \ln Z(\lambda S)}{\partial s_3} \right]$$

$$= \mathbb{I} + C_1(S) \frac{1}{\lambda} + C_2(S) \frac{1}{\lambda^2} + \dots$$
(157)

For an arbitrary $F' = USV^{\top}$, we would then have:

$$\mathbb{E}_{\mathbf{R} \sim \mathrm{MF}(\mathbf{R}; \lambda F')}[\mathbf{R}] = U \mathbb{E}_{\mathbf{R} \sim \mathrm{MF}(\mathbf{R}; \lambda S)}[\mathbf{R}] V^{\top}.$$
 (158)

D ADDITIONAL RESULTS IN PRACTICE

Here, we report the RMSD after alignment for the same training runs in Figure 4 and Figure 5. Note that our estimators are not optimal for this metric; indeed, they minimize the deviation to the optimal denoiser, not to the aligned ground truth x. The complication is that computing the optimal denoiser is not practical in a training setup.

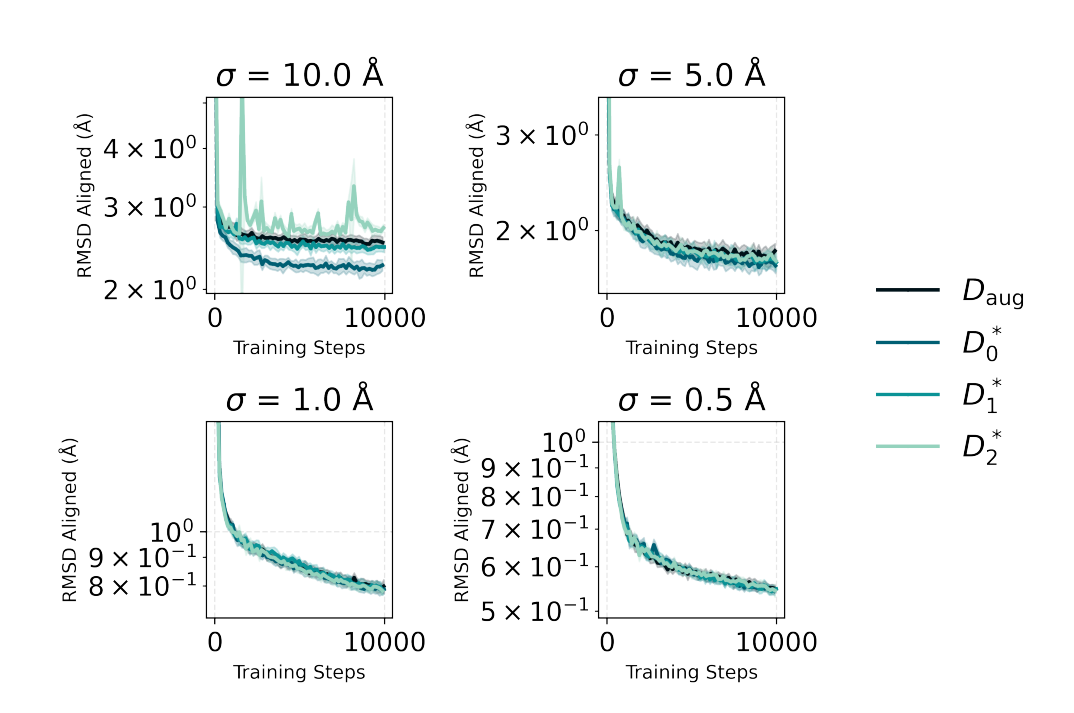


Figure 6: Training progress for the MLP, as measured by RMSD to ground-truth x after alignment, when trained using D_{aug} , D_0^* , D_1^* and D_2^* . x is sampled from all 50000 frames of a molecular dynamics simulation for the AEQN peptide.

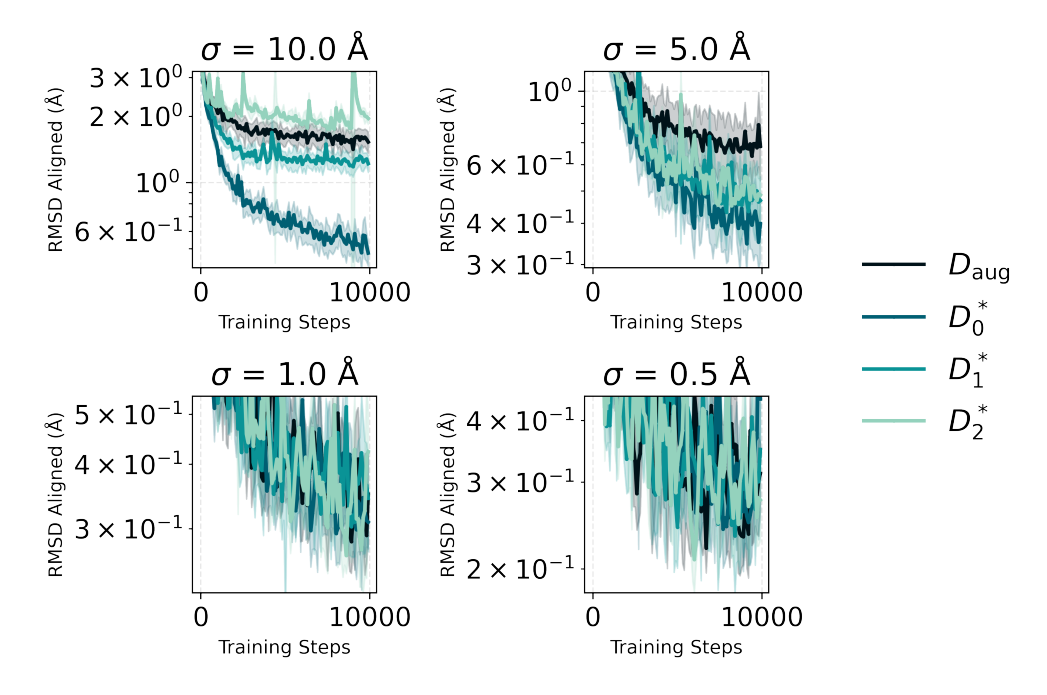


Figure 7: Training progress for the MLP, as measured by RMSD to ground-truth x after alignment, when trained using D_{aug} , D_0^* , D_1^* and D_2^* . x is fixed as the first frame in the molecular dynamics simulation for the AEQN peptide.